Targeted radiotherapy of metastatic neuroendocrine tumours

Clinical and experimental studies

Anna-Karin Elf

Department of Surgery
Institute of Clinical Sciences
Sahlgrenska Academy, University of Gothenburg

UNIVERSITY OF GOTHENBURG

Gothenburg 2018

Cover illustration by Saga Elf

“Because sometimes it is a zebra…”

Targeted radiotherapy of metastatic neuroendocrine tumours – clinical and experimental studies

Anna-karin.elf@vgregion.se

ISBN 978-91-7833-187-1 (PRINT)
ISBN 978-91-7833-188-8 (PDF)
http://hdl.handle.net/2077/57953

Printed in Gothenburg, Sweden 2018
Printed by BrandFactory

To my Dad, for sharing minds

Targeted radiotherapy of metastatic neuroendocrine tumours

Clinical and experimental studies

Anna-Karin Elf

Department of Surgery, Institute of Clinical Sciences
Sahlgrenska Academy, University of Gothenburg, Sweden

ABSTRACT

Neuroendocrine tumours (NET) often present at a metastatic stage, which diminishes the possibility for curative surgery. Peptide receptor radiotherapy (PRRT) with ^{177}Lu-DOTATATE targets somatostatin receptors, which are overexpressed on NET cells. PRRT results in symptom relief and often tumour control of NETs, but rarely cure. Tumour response is variable and renal and haematological toxicity are dose-limiting side effects.

In metastatic small intestinal NET (SI-NET) hepatic metastases are often a clinical problem. Several treatment options exist and radioembolization (RE) of the liver is a recently introduced therapy. Diffusion weighted MRI (DWI) is a new imaging technique reflecting the microenvironment of tumours and is maybe useful for treatment response evaluation.

Aims of the thesis project were to identify predictive factors for response and long-term outcome after PRRT, and investigate a possibility for radiosensitization. Further, RE was compared to hepatic artery embolization (HAE) for SI-NET hepatic metastases, and the utility of DWI as a predictor for morphologic treatment response was investigated.

A retrospective study of 51 NET patients treated with ^{177}Lu-DOTATATE revealed an objective response rate of 13%, however most patients responded with a halted tumour growth. High tumour proliferation rate, but not diagnosis, was associated with shorter survival. Overall long-term toxicity was low. The absorbed tumour dose varied considerably within and between patients, but the median absorbed tumour dose was correlated with tumour shrinkage.

In a retrospective study on stage IV SI-NET, patients with low somatostatin receptor 2 (SSTR2) expression did not have an inferior outcome after PRRT.

In contrast, a tendency was found towards both higher activity uptake after PRRT and longer survival.

In an experimental animal study, the NAMPT inhibitor GMX1778 enhanced the efficacy of ^{177}Lu-DOTATATE and almost eradicated all tumours.

In a clinical prospective study on SI-NET hepatic metastases, HAE resulted in earlier tumour shrinkage than RE, and the response at 3 months was correlated with DWI after 1 month. A low baseline apparent diffusion was correlated with a larger tumour shrinkage after 6 months.

In conclusion, tumour grade can predict long-term outcome after PRRT in metastatic NET and tumour dosimetry can be useful for response prediction. Low SSTR2 expression should not exclude patients from PRRT. GMX1778 might be used as a radiosensitizer in PRRT for SI-NET. DWI can be useful for prediction and early evaluation of treatment response after RE and HAE for liver metastasized SI-NET.

Keywords: neuroendocrine tumour, peptide receptor radionuclide therapy, somatostatin receptor 2 expression, radiosensitization, radioembolization, diffusion weighted imaging

SAMMANFATTNING PÅ SVENSKA

Neuroendokrina cancertumörer (NET) utgår från celler med förmåga att utsöndra ämnen, som kan ge hormonellt orsakade tillstånd och symptom såsom diarré, värmevallningar, magsår och blodsockersvängningar. När tumörerna har spridit sig till lymfkörtlar och lever, går sjukdomen inte längre att bota med kirurgi. Receptor-medierad strålbehandling (PRRT) med den radioaktiva isotopen Lutetium-177 (^{177}Lu-DOTATATE) riktar sig mot somatostatin-receptorer (SSTR), som finns på cellytan av de flesta NET. Tumörerna är generellt långsamväxande, vilket gör att strålbehandling ofta har begränsad effekt, men PRRT har visats förlänga överlevnaden hos patienter med spridd NET. Behandlingen, som ges intra-venöst, ger symptomlindring och bromsar tumörtillväxten, men leder sällan till bot. Behandlingseffekten av PRRT varierar och man vet fortfarande ganska lite om vilka faktorer som påverkar utfallet. PRRT ger också dosberoende biverkningar i form av försämrad funktion av njurar och benmärg p.g.a. att även normalvävnad bestrålas.

Vid NET med ursprung från tunntarmen (SI-NET) utgör levermetastaserna ofta ett kliniskt bekymmer, eftersom de är många och kan bli mycket stora, och därigenom orsakar de svåra hormonella symptom. Behandling riktad specifikt mot levern är att föredra, eftersom sådan inte påverkar njur- och benmärgsfunktionen, som systembehandlingar kan göra. Levertumörer får sitt blod huvudsakligen via lever-pulsådern och genom att ge behandling direkt i denna får man inte så mycket påverkan på den friska levervävnaden, som huvudsakligen försörjs vi porta-venen. Radioembolisering (RE) via lever-pulsådern är en ny strålbehandling med mikrosfärer innehållande den radioaktiva isotopen Yttrium-90 och utövar effekt genom stålning. Leverartärembolisering (HAE) är en beprövad metod, som ger infarkt i levertumörerna genom att blodflödet i lever-pulsådern stängs av med insprutade partiklar. Behandlingsutvärdering görs vanligen med datortomografi, men magnetkamera med diffusionsviktade bilder (DWI) är en ny avbildningsmetod, som avspeglar mikromiljön i tumörerna.

Syftet med delstudie I-II var att hitta faktorer som skulle kunna förutsäga behandlingssvar och långtidsresultat hos 51 patienter, som erhöll PRRT 2006 till 2011 på Sahlgrenska Universitetssjukhuset. Syftet med delstudie III var att undersöka om SI-NET kunde göras mer känsliga för PRRT genom kombinationsbehandling med GMX1778. Syftet med delstudie IV var att jämföra RE med HAE och studera om DWI kan användas för tidig behandlingsutvärdering och för att förutsäga behandlingssvar.

I första delstudien såg vi att få tumörer krympte signifikant av PRRT men de flesta tumörers tillväxt avstannade. En hög tillväxthastighet (proliferation) i tumörcellerna ledde till snabbt återfall och kortare överlevnad för dessa patienter. Långtidsbiverkningarna av PRRT var få. Den absorberade stråldosen i tumörerna varierade kraftigt mellan tumörer inom och mellan patienter. Vi kunde påvisa ett samband mellan absorberad median-tumördos och storleksminskning av tumörerna.

I den andra delstudien undersöktes SI-NET-tumörer mikroskopiskt, varpå vi fann att de flesta tumörer uttryckte en hög nivå SSTR subtyp 2. Patienter med tumörer med lågt SSTR2-uttryck hade en tendens till högre upptag av radioaktivitet vid PRRT, vilket var överraskande. Dessutom hade de en tendens till längre överlevnad, vilket var motsatt vår hypotes.

Den tredje delstudien var en experimentell modell med human SI-NET, där PRRT-behandlade möss även fick GMX1778, som hämmar ett enzym i processen att återskapa NAD^+. NAD^+ är ett ko-enzym som är centralt för cellers energitillverkning och det förbrukas vid strålskada. Kombinations-behandlingen förstärkte effekten av PRRT och resulterade i att tumörerna nästan försvann helt, utan någon annan effekt på mössen.

Den fjärde delstudien var en prospektiv jämförande behandlingsstudie på patienter med levermetastaser från SI-NET. HAE gav tumörkrympning tidigare än RE, men efter 6 månader sågs inte längre någon säker skillnad mellan behandlingarna. Ökning av diffusion mätt med DWI en månad efter behandling korrelerade med tumörkrympning vid 3 månader. Lågt diffusionsvärde innan behandling korrelerade med tumörkrympning vid 6 månader.

Slutsatser som kan dras är att PRRT är en väl tolererad behandling, där tumörens proliferationsgrad korrelerar med överlevnad. Tumördosimetri kan vara användbar för att förutsäga behandlingssvar. Lågt SSTR2-uttryck bör inte exkludera patienter från PRRT. GMX1778 kan möjligen användas för radiosensibilisering vid PRRT för SI-NET. DWI kan vara användbar för att förutsäga och tidigt utvärdera behandlingssvar efter RE och HAE vid levermetastaserad SI-NET.

THESIS AT A GLANCE

Paper	Questions	Methods	Results	Conclusions
I	Can predictive factors be identified for long-term outcome or toxicity after PRRT (^{177}Lu-DOTATATE)? Is the absorbed tumour dose predictive of morphological tumour response?	Retrospective descriptive study on our first 51 patients treated with ^{177}Lu-DOTATATE. RECIST and biomarker evaluation. Long-term follow-up with PFS and OS. Tumour dosimetry using planar scintigraphy and SPECT after treatment.	The PFS and OS was similar regardless of NETdiagnosis, but patients with G3 tumours had a shorter PFS and OS than those with G1 and G2 tumours. Side effects were few. In a heterogeneous NET cohort a correlation was found between median absorbed tumour dose and tumour shrinkage.	For evaluation of metastatic NET after ^{177}Lu-DOTATATE, Ki-67 is a stronger predictive marker for long-term outcome than tumour origin. Tumour dosimetry is feasible and seems to correlate with tumour shrinkage, however large variations were seen within and among patients.
II	Can low SSTR2 expression predict a worse outcome after ^{177}Lu-DOTATATE? Is the radioactivity uptake lower in tumours with low SSTR2 expression?	IHC analysis of TMA block for SSTR2 and Ki-67 compared with OS in SI-NET patients treated with ^{177}Lu-DOTATATE. Measurement of activity concentration in SPECT 24h after PRRT.	SI-NET patients with low expression of SSTR2 did not have a shorter OS after PRRT, compared to patients with high expressing tumours. Nor did they have a lower radioactivity uptake at 24h SPECT.	The expression of SSTR2 cannot predict long-term outcome after ^{177}Lu-DOTATATE for metastasized SI-NET, hence patients with low expression should not be excluded from PRRT.
III	Can NAMPT inhibitor GMX1778 be used as a radiosensitizer in SI-NET?	Experimental study with nude mice xenografted with SI-NET followed for 17 weeks. Measurement of tumour size, time to tumour progression.	Combining a low dose of GMX1778 with a low dose of ^{177}Lu-DOTATATE resulted in substantially reduced tumour volumes and a prolonged time to tumour progression.	GMX1778 enhances the tumour reducing effect of ^{177}Lu-DOTATATE and prolongs time to tumour progression. Hence, GMX1778 can be used as a radiosensitizer for PRRT.
IV	Is there a difference in treatment outcome after HAE and RE? Can DWI be an early predictor of treatment response in SI-NET hepatic metastases?	Prospective study randomizing to HAE or RE with ^{90}Y. RECIST and biomarker evaluation. Baseline and 1-month DWI compared with MRI 3 and 6 months.	Patients treated with HAE had initially a better tumour response, but at 6 months the response was similar for both treatments. A low baseline and high increase of 1-month DWI correlated with pronounced tumour shrinkage.	At 6 months, the response is similar after HAE and RE. Early measurement of the apparent diffusion coefficient (ADC) seems to predict tumour response.

PFS=progression-free survival, OS=overall survival, NET=neuroendocrine tumour, PRRT=peptide receptor radionuclide therapy, SSTR2=somatostatin receptor type 3, IHC=immunohistochemical, SI-NET=small intestinal NET, HAE=hepatic artery embolization, RE=radioembolization, DWI=diffusion weighted imaging

LIST OF PAPERS

This thesis is based on the following studies, referred to in the text by their Roman numerals.

I. **Treatment with ^{177}Lu-DOTATATE for metastasized neuroendocrine tumours – long-term effects and a tumour dosimetry model.** Elf AK, Marin I, Rossi Norrlund R, Svensson J, Wängberg B, Nilsson O, Bernhardt P, Johanson V.

In manuscript

II. **Can SSTR2 expression in previously resected SI-NETs predict overall survival after PRRT treatment of remaining lesions?** Elf AK, Johanson V, Marin I, Bergström A, Nilsson O, Svensson J, Wängberg B, Bernhardt P, Elias E.

In manuscript

III. **NAMPT inhibitor GMX1778 enhances the efficacy if ^{177}Lu-DOTATATE treatment of neuroendocrine tumours.** Elf AK, Bernhardt P, Hofving T, Arvidsson Y, Forsell-Aronsson E, Wängberg B, Nilsson O, Johanson V.

Journal of Nuclear Medicine 2017; 58(2):288-292

IV. **Radioembolization Versus Bland Embolization for Hepatic Metastases from Small Intestinal Neuroendocrine Tumors: Short-term Results of a Randomized Clinical Trial.** Elf, AK, Andersson M, Henriksson O, Jalnefjord O, Ljungberg M, Svensson J, Wängberg B, Johanson V.

World Journal of Surgery 2018; 42:506-513

CONTENTS

ABBREVIATIONS

5-HIAA	5-hydroxyindoleacetic acid (SI-NET biomarker)
^{99m}Tc-MAA	Technetium-99m macroaggregated albumin
ADC	Apparent diffusion coefficient
BR	Best response
CgA	Chromogranin A (NET biomarker)
CR	Complete response
CT	Computed tomography
DWI	Diffusion weighted imaging
EUS	Endoscopic ultrasound
G1-G3	Proliferation grade 1-3
GEP-NET	Gastro-entero-pancreatic neuroendocrine tumour
GFR	Glomerular filtration rate (renal function)
HAE	Hepatic artery embolization
IHC	Immunohistochemistry
Ki-67	Tumour proliferation marker
LD	Longest diameter
MRI	Magnetic resonance tomography
NAD^+	Nicotinamide adenine dinucleotide
NET	Neuroendocrine tumour
OS	Overall survival

Pan-NET	Pancreatic neuroendocrine tumour
PD	Progressive disease
PET	Positron emission tomography
PFS	Progression-free survival
PR	Partial response
PRRT	Peptide receptor radionuclide therapy
RE	Radioembolization
RECIST	Response evaluation criteria in solid tumours
RILD	Radiation induced liver disease
ROI	Region of interest
SD	Stable disease
SI-NET	Small intestinal neuroendocrine tumour
SPECT	Single-photon emission computed tomography
SRS	Somatostatin receptor scintigraphy
SSA	Somatostatin analogue
SSTR	Somatostatin receptor
TMA	Tissue microarray
VOI	Volume of interest

INTRODUCTION AND BACKGROUND

This doctoral thesis focuses on outcome after receptor-mediated radionuclide therapy of neuroendocrine tumours (NETs), especially small intestinal and other gastro-entero-pancreatic NETs (SI-NETs and GEP-NETs), and explores radiosensitization as a way to increase the efficacy of the treatment. It also compares radioembolization to traditional bland embolization as a treatment for SI-NET hepatic metastases and investigates diffusion weighted MRI as an evaluation method.

NEUROENDOCRINE TUMOURS

Neuroendocrine tumours (NETs) arise from neuroendocrine cells situated in various tissues in the body (1). The most common types are broncho-pulmonary and gastro-entero-pancreatic tumours (GEP-NETs) (2). Clinical presentation depends on the cell type and site of the primary tumour, and whether they are functioning tumours, *i.e.* hormone producing with specific hormonal symptoms. Among metastasized GEP-NETs, SI-NET is the most common diagnosis, characterized by its overproduction of serotonin. A large tumour burden can cause the classical carcinoid syndrome with diarrhoea, cutaneous flushing and abdominal pain as cardinal symptoms, together with right-sided heart valve dysfunction. The neuroendocrine pancreatic tumours (pan-NETs) are often non-functioning, which leads to a late clinical presentation with mass effect, such as diffuse abdominal pain, as the predominant symptom. The late detection can also result in a higher stage with distant metastases at diagnosis. The functioning pan-NETs cause symptoms at an earlier stage, *e.g.* hypoglycaemia (insulinomas) and recurrent peptic ulcers (gastrinomas).

The incidence of NETs is about 2.5-5/100000, but the prevalence is much higher due to their mostly slow growing nature, which gives the patients a fairly long survival (2-5). The incidence has increased substantially during the last decades, as described in the SEER database (6). This is probably due to more frequent and more sensitive radiological and endoscopical examinations, as well as refined histopathology.

Diagnosis

The slow progression of NETs leads to an indolent course and delayed diagnosis at an already advanced stage. Almost half of all SI-NETs are diagnosed in an acute setting due to intestinal obstruction and impaired circulation. This is caused by primary tumours or mesenteric lymph node metastases together with the typical desmoplastic reaction often associated with SI-NETs (7).

When a suspicion of neuroendocrine tumour is raised, biochemical screening should be performed together with imaging. This includes the general NET marker chromogranin A (CgA), together with site-specific hormones or their metabolites, *e.g.* dU-5-HIAA in SI-NETs (8).

Detailed staging is necessary for proper management and is reached by the combination of computed tomography (CT) or magnetic resonance imaging (MRI) and functional imaging of somatostatin receptors (SSTR) (see SSTR chapter). CT and MRI typically show contrast enhancement due to the rich vascularization of NET.

Another useful diagnostic tool, especially in upper gastro-intestinal and pan-NETs, is endoscopic ultrasound (EUS) (9). In hereditary syndromes with multiple tumours, the lesions are sometimes very small and can be difficult to localize with CT or MRI. EUS is then a more sensitive imaging modality, and does not expose the patient to radiation, which is advantageous when repeated exams are needed. Furthermore, the EUS technique enables obtaining a biopsy with good precision (10).

The definite diagnosis is established with a tumour biopsy, which is immunohistochemically (IHC) stained for CgA, synaptophysin and relevant hormones (Fig. 1). Proliferation rate for grading is revealed by the mitotic count and/or the Ki-67 index, using the MIB1 antibody (11). A tumour biopsy cannot always be obtained preoperatively. Then imaging and convincing biomarkers can be enough for the decision to operate.

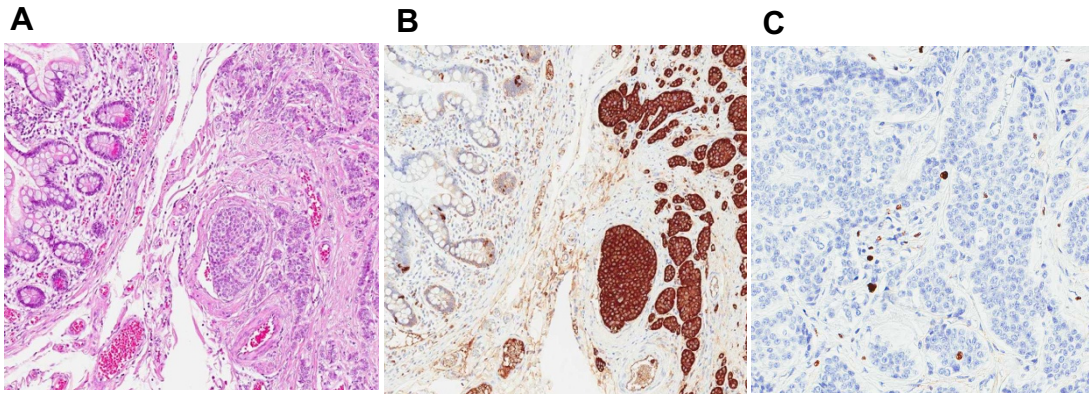

Figure 1. Micrographs of SI-NET. A. *Histopathological staining with hematoxylin-eosin.* ***B.*** *Immunohistochemical (IHC) staining for Chromogranin A visualizes neuroendocrine cells, mainly located in the tumour.* ***C.*** *IHC staining for Ki-67 with the antibody MIB1 reveals tumour proliferation rate.*

Classification, staging and grading

NETs are at diagnosis classified by two parameters: stage and grade. These are important prognostical factors for long-term outcome in NETs (6, 12, 13). The tumour-node-metastasis (TNM) classification is used, and stage is of great importance for planning of treatment for the patient (14). T is determined by the size and infiltration depth of the primary tumour, N and M are determined by the presence of regional lymph node and distant metastases, respectively. The anatomical extent of the disease is the classified into stage I-IV, where stages III and IV are mainly defined by the presence of lymph node and distant metastases.

Grade	Mitotic count per 10 HPF	Ki-67 index* (%)
G1	≤ 2	< 3
G2	2 - 20	3 - 20
G3	> 20	> 20

Table 1. Grading of gastroenteropancreatic neuroendocrine neoplasias. *HPF = high-power fields, * MIB1 antibody: per cent of 500-2000 cells (15)*

The European Neuroendocrine Tumour Society (ENETS) has developed a histopathological grading system with three categories (G1, G2, G3), based on Ki-67 index and mitotic count (Table 1) (15).

Most common are G1 and G2 tumours, which have a significantly better prognosis than G3. However, G3 tumours are a heterogeneous group, and they are often divided in G3 NET (lower Ki-67 range) and G3 NEC (neuroendocrine carcinoma) (Ki-67>55%). G3 NETs are treated similarly to G2 tumours, but G3 NECs have a significantly worse prognosis, often necessitating other treatments than G1, G2 and G3 NETs. In newer terminology all G1-G3 tumours are referred to as neuroendocrine neoplasias (NEN), which include both NETs and NECs.

TREATMENT OF GEP-NETS

GEP-NETs constitute a very heterogeneous group of tumours, from small gastric and rectal NETs to metastasized, fast growing G3 NECs. In a nationwide Swedish register study including all kinds of NENs from all sites, 23% were metastatic. Small intestinal and pancreatohepatobiliary (mostly pancreatic) NENs carried the highest proportion of metastases, 41% and 58%, respectively. Appendiceal and rectal NENs were rarely metastastic, 3% and 13%, respectively. Colon and gastric NENs had metastases in 18% and 31%, respectively (16). Obviously, the treatments are as diverse as the tumours. Here, mainly treatments of G1 and G2 SI-NETs and pan-NETs are discussed.

Surgical treatment

Incidentally discovered GEP-NETs, when the disease is loco-regional and before start of hormonal symptoms, are treated with a curative intent. In SI-NETs, a bowel resection with regional lymphadenectomy is usually performed, resulting in an excellent prognosis with a 5-year survival of 100% for stage I and II and 97% for stage III disease (17-19). In stage IV disease (distant metastases present) resection of the primary tumour and lymph nodes are usually resected, however the long-term benefit of this has been questioned (20). In pan-NETs, the stage and grade are important prognostic factors for long-term outcome (21-24), and are also used as a guide to timing of surgery. For non-functional, small G1 tumours an active surveillance approach could be applied, with repeated radiological follow-up examinations. For larger (> 2

cm) or G2 tumours resection is recommended (25). Furthermore, the localization of the tumour is of great importance, since the surgical procedures have different side effects and complication rates, depending on if the caput (Whipple's procedure) or the cauda (laparoscopic tail resection) is resected. A functioning tumour most often leads to a pancreatic resection up-front, due to the hormonal symptoms.

Systemic treatment

Since NETs are often metastasized when symptoms occur, the treatment is commonly multimodal with a palliative intent. Beside somatostatin receptor mediated therapies (see SSTR chapter), chemotherapy, oncogenic pathway inhibitors and interferon-α have been used.

In G3 tumours, chemotherapy is an important part of the multimodal approach for localized disease and the mainstay of treatment in advanced or metastatic disease (26). Generally, platinum-based chemotherapy is used in combination with etoposide. For G2 NETs in higher range and G3 tumours in the lower range temozolamide and capecitabine could be considered (26).

In recent years, molecular targeted therapies have been introduced for treatment of NETs. These therapies include the mTOR inhibitor everolimus and the tyrosine kinase inhibitor sunitinib. Everolimus has been compared to placebo in a large randomized controlled study on advanced G1-G2 NETs, showing a prolonged progression-free survival (PFS) in favour of everolimus (11 versus 3.9 months) (27). Sunitinib has been investigated for well-differentiated (G1-G2) pan-NETs in another placebo-controlled study. The study was discontinued early after 22 months due to more adverse events and deaths in the placebo group as well as a difference in PFS favouring sunitinib (11.4 versus 5.5 months) (28). Indeed, these are convincing results, but in both of these studies the control groups were left with only placebo treatment, something that rarely is the case in the clinic.

TREATMENT OF HEPATIC METASTASES

The liver is the main site for distant metastases in GEP-NETs, and the presence of hepatic metastases influences the prognosis (29). These metastases can be large and extensive, and they are the main source for hormonal symptoms. In SI-NETs, secretory products from the primary tumours and regional lymph

nodes follow the portal vein blood and are metabolized in the liver, while tumour products from hepatic metastases are secreted directly into the systemic circulation, giving rise to the carcinoid syndrome. A number of treatment alternatives have been introduced for hepatic metastases.

Surgical resection

The primary tumour and regional lymph node metastases can often be resected radically. Surgery is also the treatment of choice for G1 and G2 hepatic NET metastases if a complete resection of liver metastases could be performed safely (29-31). In this setting, surgical intervention has in retrospective studies shown a survival benefit compared with less aggressive (non-surgical/pharmacological) treatment (32, 33). For selected patients, liver transplantation can be a treatment option (34, 35).

Non-surgical therapy

In most cases, the hepatic metastases are widely spread or the patient have co-morbidities making surgical resection unsuitable. In patients with predominantly hepatic tumour burden, a liver-directed regional treatment is a preferable alternative, since systemic adverse reactions, *e.g.* haematological toxicity and other side effects from chemotherapy, oncogenic pathway inhibitors and interferon-α, can be avoided. These non-surgical treatments are considered palliative and include ablation and trans-arterial embolization of hepatic metastases. They result in symptomatic relief and often tumour regression, but no differences between treatments regarding long-term outcome have been confirmed in meta-analyses (31, 36, 37). Factors affecting the choice of method mainly regard severity of disease and distribution of metastases.

Ablation

Ablation of hepatic metastases is accomplished by radiofrequency, microwave or laser techniques. All techniques induce hyperthermia and can be performed percutaneously or intra-operatively with sonographic guidance. The treatment has a high tolerability and side effects are rare and mainly related to the electrode placement (38, 39). In SI-NETs, ablation can lead to decreased

biomarkers and delayed tumour progression, but OS is probably not prolonged (40).
Ablative procedures necessitate treatment of metastases individually, which limits the number of metastases that can be treated at one occasion. Not all metastases can be visualized on the pre-therapeutic ultrasound, and for technical reasons, larger metastases cannot be treated. Further, metastases located adjacent to the diaphragm, heart or bile ducts are unsuitable for percutaneous treatment, due to the heat dispersion from the ablative procedure. In metastases close to larger vessels it is difficult to achieve hyperthermia due to the cooling effect of the blood flow.

Embolization

Neuroendocrine tumours are highly vascularized with their main blood supply from the hepatic artery, while the liver parenchyma is perfused mainly by the portal vein. By embolization via the hepatic artery a certain degree of tumour specificity of the treatment can be achieved (41). Trans-arterial embolization can be performed using three different strategies (Fig. 2). The side effects differ between treatments and vary depending on their different way of acting.

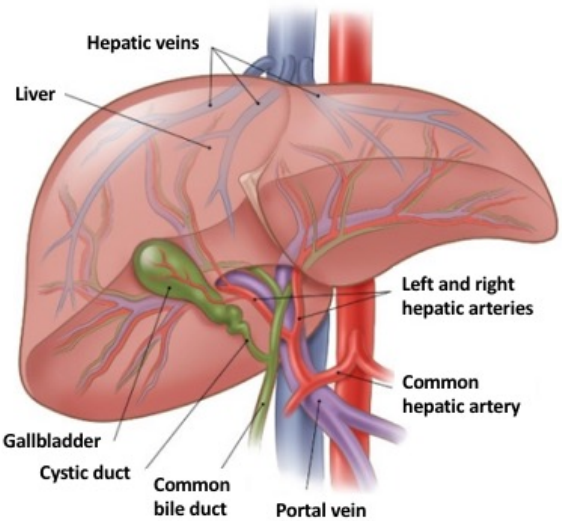

Figure 2. ***Embolization of liver.*** *Via a catheter inserted in the right femoral artery, the right or left hepatic artery branches (in HAE or HACE) or the common hepatic artery (in RE) are reached, where the embolization treatment is deposited. Normal liver tissue is perfused mainly via portal vein, and is spared from the embolization treatment. Illustration from American Cancer Society.*

Hepatic artery embolization (HAE), or bland embolization, using polyvinyl alcohol (PVA) particles or gelatine foam, aims to completely block the circulation in the hepatic artery, which induces tumour ischemia and necrosis. (42). The treatment is divided into two sessions approximately six weeks apart, treating one lobe at a time to avoid serious side effects. Nevertheless, main side effects are related to ischemia and include abdominal pain, nausea, fever and transiently increased hepatic enzymes. Rarely, hepatic abscesses and hepatorenal syndrome are seen (43).

In hepatic artery chemoembolization (HACE) the procedure is similar, but streptozotocin or doxorubicin is added. This gives a regional cytotoxic effect to the embolization, but at much higher levels than systemic chemotherapy (44). A wider spectrum of side effects is also seen, compared with HAE.

Radioembolization (RE) is aiming not for ischemia but for a tumour selective deposition of radiolabelled microspheres (^{90}Yttrium), hence an internal radiotherapy. The particle size is significantly smaller and amounts much less than in HAE, which avoids ischemic side effects and the whole liver can be treated at once. Common side effects described after RE are abdominal discomfort and fatigue for some weeks (45, 46). Usually patients are discharged on the day after treatment, in contrast to patients receiving HAE, who need median 4 hospital days after treatment (43).

HAE and HACE often result in reduced biomarkers, symptom relief and tumour regression (47), and maybe an improved long-term outcome in responding patients (48, 49). Furthermore, RE is described to result in effective disease control and improved quality of life (50).

There are only few studies comparing the different embolization therapies, and these are often retrospective, introducing bias. Included patients are often heterogeneous regarding tumour origin and grade, which complicates evaluation and makes it difficult to draw firm conclusions. For SI-NETs, there seems to be no benefit with HACE compared with HAE, but maybe for p-NETs (51). However, HACE seems to be more toxic than HAE (52). In a small retrospective study on both HAE, HACE and RE no differences between PFS or overall survival (OS) was seen between the groups (53).

SOMATOSTATIN RECEPTORS

Somatostatin receptors (SSTR) are G-protein coupled receptors that are normally expressed in many tissues in the body, including the gastrointestinal tract, kidneys, pancreas and nervous system. Five major receptor subtypes are identified (1-5) and they are overexpressed in many NET cells. SSTR2 is the subtype most commonly overexpressed by GEP-NETs (54, 55). To some extent, SSTR1 and SSTR5 are also overexpressed. When the receptor is activated by the endogenous ligands somatostatin-14 and -28, an inhibition of gastrointestinal motility, endocrine and exocrine secretion via intracellular cAMP and Ca^{2+} connected pathways (56).

Somatostatin analogues

Octreotide, the first somatostatin analogue (SSA), was synthesized more than 3 decades ago by the chemist Wilfried Bauer (57). This synthetic peptide has an increased inhibitory activity and prolonged duration of action, compared with natural somatostatin. It has a high affinity for SSTR2 and moderate affinity for SSTR3 and SSTR5, making it ideal in the treatment of GEP-NETs (56). Other SSAs have been synthesized, where the most important are lanreotide, with similar SSTR affinities as octreotide, and pasireotide, with affinity for SSTR5 and SSTR1-3 (58, 59).

Octreotide has been used clinically for many years for its symptom-reducing effect on hormone secreting NETs (60). Occasionally, a reduction of tumour progression was also seen, and this anti-proliferative effect has been confirmed in two large studies with long-acting SSA, PROMID and CLARINET (61, 62), where octreotide and lanreotide was compared with placebo. These studies showed that PFS was significantly longer for the patients with SSA treatment, but no difference in overall survival could be demonstrated. The lack of survival benefit was however not unexpected, since placebo treated patients were allowed to cross-over to SSA at tumour progression.

Somatostatin receptor mediated imaging

Somatostatin receptors are also used for diagnosis of NETs. SSTR-positive tumours are visualized by imaging using radiolabelled SSA and scintigraphy or positron emission tomography (PET). This type of imaging was first performed by using an iodine radionuclide (^{123}I), but soon ^{111}In was established as the preferable isotope due to better physical and metabolic properties (63). ^{111}In is connected via the chelating agent diethylene triamine pentaacetic acid

(DTPA) to octreotide, which is readily bound to the SSTR. As ^{111}In emits gamma rays, SSTR positive tumours can be visualized by a gamma camera, *i.e.* somatostatin receptor scintigraphy (SRS).

This technique has been used for many years as an important tool for diagnosis, staging and treatment evaluation of NETs. However, the low sensitivity for small and certain types of lesions has been an issue for concern. In more recent years the positron emitting radionuclide ^{68}Ga has been labelled to somatostatin analogues, *e.g.* ^{68}Ga-DOTATATE, enabling the use of positron emission tomography (PET) for visualization. This imaging technique has emerged as a more sensitive imaging method (64, 65). It is often combined with a low-resolution CT (PET/CT) to obtain 3D anatomical images.

Somatostatin receptor mediated therapy

The radionuclide ^{111}In is mainly a gamma emitter, making it well suitable for tumour detection in a gamma camera. Since it also emits high linear energy transfer Auger electrons, it was initially investigated for radiotherapeutic use in NETs (66, 67). This peptide receptor radionuclide therapy (PRRT) lead to symptomatic relief and biomarker decrease, but tumour shrinkage was rarely observed. Further, the high activity amounts needed for therapy entailed substantial levels of gamma radiation, with radioprotective concerns as a consequence.

Many radionuclides have been theoretically and experimentally investigated for their feasibility as radiopharmaceuticals in PRRT (68, 69). The most commonly used radionuclide is ^{131}I for therapy of thyroid diseases. For somatostatin receptor mediated radiotherapy, ^{177}Lu and ^{90}Y are the most frequently used radionuclides, which have appropriate radio-physical characteristics for treatment purposes, and are also suitable for industrial production (Table 2).

	Type of decay	Range (max; mm)	Half-life (days)
^{111}In	EC, γ	Short range	2.8
^{177}Lu	ß, γ	2	6.7
^{90}Y	ß	11	2.7

Table 2. Physical properties of radionuclides used in PRRT*. EC= electron capture*

The short range of ^{177}Lu affects tumour cells in close proximity, theoretically sparing the normal tissue. ^{177}Lu also emits gamma radiation, which facilitates detection and quantification using gamma cameras. The longer range of ^{90}Y enables an effective treatment of larger tumours, and possibly compensates for uneven distribution of the radioactivity. However, the long range is also a disadvantage when treating an abundance of small hepatic metastases (diameter <1 mm) (70), and the renal function is more often affected than with ^{177}Lu (71, 72). Furthermore, its exclusive ß emitting decay complicates post-injection detection with gamma cameras.

In order to direct the radionuclide to the tumour, it is bound via a chelator to the peptide, which in turn acts as a ligand to the SSTR. Improvement of PRRT has included development of new chelating agents as well as peptides. The chelator dodecane tetraacetic acid (DOTA) has superior biodistributive and stabilizing characteristics compared with DTPA (73). The binding of the radionuclide-ligand complex was improved when introducing the peptide octreotate, which has a higher affinity for the SSTR2 (74, 75).

^{177}LU-DOTATATE TREATMENT

The most commonly used radio-pharmaceutical in PRRT is ^{177}Lu-DOTATATE, consisting of ^{177}Lu coupled to octreotate with the chelator DOTA. The treatment is usually divided into fractions of 7.4 GBq given as an intravenous infusion during 30 minutes (76-80). To prevent the uptake in the kidneys, infusions of the positively charged amino acids lysine and arginine are administered concomitantly, starting 30 minutes before the ^{177}Lu-DOTATATE infusion is initiated (81). Patients recover quickly after treatment

and the hospital stay surrounding therapy is mainly indicated for radiation protection reasons.

After treatment patients are monitored with blood sampling, to determine the renal and haematological impacts. A biokinetic and dosimetric evaluation of the radiopharmaceutical is usually performed with repeated planar scintigraphy and/or single-photon emission computed tomography (SPECT).

The treatment fractions are repeated every 6 to 10 weeks, allowing for the recovery of bone marrow and kidneys between fractions. Since renal side effects constitute one of the main clinical concerns, the renal uptake often determines how much radiation that can be delivered. In a commonly used clinical protocol for PRRT, fractions are repeated up to 4 times, unless the renal dose limit of 23-28 Gy is exceeded (80, 82).

Effect of ^{177}Lu-DOTATATE

Peptide receptor radionuclide radiotherapy is a palliative treatment often resulting in halted tumour progression or shrinkage of the tumour, but very rarely cure. The tumour response of ^{177}Lu-DOTATATE is highly variable with objective response rates between 24 and 36%, and progressive disease between 3 and 20% (76, 83-85). Different NETs seem to respond differently to the treatment. Other important effects are symptom relief and improvement of quality of life for patients (84, 86).

In animal studies complete remission of tumour has been demonstrated with escalated doses (87), but in humans the side effects are dose-limiting (84). Clinical dose-response investigating studies are few, but in a recently published study by Garske et al. a renal dose-driven protocol was proposed (85). A correlation was described between radiological tumour response and absorbed dose to the kidneys, indicating a better treatment effect when a high kidney dose was achieved. It has also been demonstrated that ^{177}Lu-DOTATATE improves long-term outcome. In a large prospective study (NETTER-1) ^{177}Lu-DOTATATE was superior compared to high-dose SSA when evaluating radiological response rate, PFS and possibly OS (88).

Side effects of ^{177}Lu-DOTATATE

Treatment with ^{177}Lu-DOTATATE is generally well tolerated by patients, with only mild side effects associated with the treatment administration. The most commonly described side effects are nausea and abdominal discomfort.

A more serious side effect is the renal radiotoxicity (77, 80). The radiopharmaceutical is eliminated by renal excretion which involves glomerular filtration, but due to tubular reabsorption a renal retention of the radioactivity occurs. Renal radiotoxicity was more pronounced before concomitant amino acid infusion became a clinical praxis (89), but decreased renal function after PRRT is still one of the major clinical concerns. The initial dose limit to the kidneys was based on the extrapolation from obtained toxicity with external irradiation (90) and was set to 23 Gy. Since then, the absorbed dose levels and the toxicity profile have been investigated and different maximum levels to avoid decreased renal function have been advocated. Bodei et al. proposed that 28 Gy seems to be a safe biological effective dose (BED) for patients with risk factors for renal impairment (co-morbidities such as hypertension and diabetes), and 40 Gy for patients without risk factors (71).

Haematological toxicity is another important side effect of PRRT. A transient decrease in platelet and leukocyte count is often observed, but patients usually recover between treatment fractions (78). Occasionally, a persistent bone marrow depression has to be managed by extended intervals between fractions, but in some patients the haematological toxicity is more severe (77). A correlation between an inferior renal function and increased haematological toxicity has been demonstrated, which has partly been explained by the prolonged circulation time of ^{177}Lu-DOTATATE due to the decreased renal excretion (80, 91).

RADIOBIOLOGY ASPECTS

Radiotherapy has since long been an important and integrated part of many cancer treatment regimes and aims predominantly to induce DNA damage in tumour cells resulting in halted proliferation or cell death.

The radiosensitivity of a cell varies depending on cell cycle phase, where cells in mitotic (M) and G_2 phases are more radiosensitive than cells in non-mitotic phases G_0/G_1 and S (Fig. 3). Rapidly dividing tumour cells have less time to repair DNA damages, making them more susceptible to the damaging effects of radiation. Furthermore, many cancer cells have defective DNA repair

systems, and a failure of DNA repair or to halt mitosis despite unrepaired DNA lead to cell death (92, 93). However, most NETs are proliferating slowly, much slower than *e.g.* the intestinal mucosa, implying a relative radioresistance.

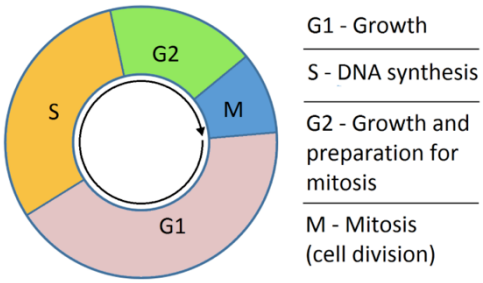

Figure 3. Phases of the cell cycle. *M and G2 phases are more sensitive to radiation than G1 and S phases. Illustration by Simon Caulton.*

Ionizing radiation can induce cellular death in several ways (94). Apoptosis, necrosis, mitotic catastrophe and cellular senescence are common ways of cellular death induced by irradiation. The DNA is the main target of radiation therapy. The ionizing radiation damages DNA directly (direct action causing strand breaks, base damages and cross-links) and ionizes water molecules, producing highly reactive free radicals ($OH^{\bullet}$, $H^{\bullet}$, e^{-}_{aq}), which damage DNA indirectly via biomolecular ionization. A radiation dose of 1 Gy is considered to induce approximately 1000 single strand breaks, 40 double strand breaks, 3000 base damages and 100 000 ionizations in a cell (95).

Upon DNA damage, different DNA repair mechanisms are activated depending on type of damage. To initiate DNA repair, the DNA damage must be recognized by the cell. One of the best studied proteins with DNA-damage scanning activity is the nuclear enzyme poly(ADP-ribose) polymerase 1 (PARP-1) (96). At a site of DNA-strand breakage, PARP-1 is activated and catalyses the transfer of ADP-ribose moieties from its substrate nicotinamide adenine dinucleotide (NAD^{+}) to nuclear proteins and histones. By modifying the architectural proteins close to the DNA breaks, the condensed chromatin structures are opened, making them more accessible to DNA repair enzymes (97). This beneficial effect of PARP-1 can also be deleterious for the cell. NAD^{+} serves not only as a substrate during ADP ribosylation, but is also a coenzyme involved in several redox reactions, including adenosine triphosphate (ATP) generation. Thus, after massive DNA damage the increased PARP-1 mediated NAD^{+} consumption can lead to depletion of ATP energy stores and cellular death (96).

NAD^+ salvage pathway

However, NAD^+ is normally resynthesized via the NAD^+ salvage pathway, which under normal circumstances ensures sufficient intracellular levels of NAD^+. The NAD^+ salvage pathway (Fig. 4) involves a few enzymes, of which nicotinamide phosphoribosyl transferase (NAMPT) is considered rate-limiting (96). The pyridyl cyanoguanidine GMX1778 has been demonstrated to inhibit NAMPT and induce cell death by depleting intracellular NAD^+ stores (98). GMX1778, formerly known as CHS828, has also been used as an anti-tumour treatment in animal studies (99). Furthermore, NAMPT inhibition has been suggested as a radiosensitization strategy (100).

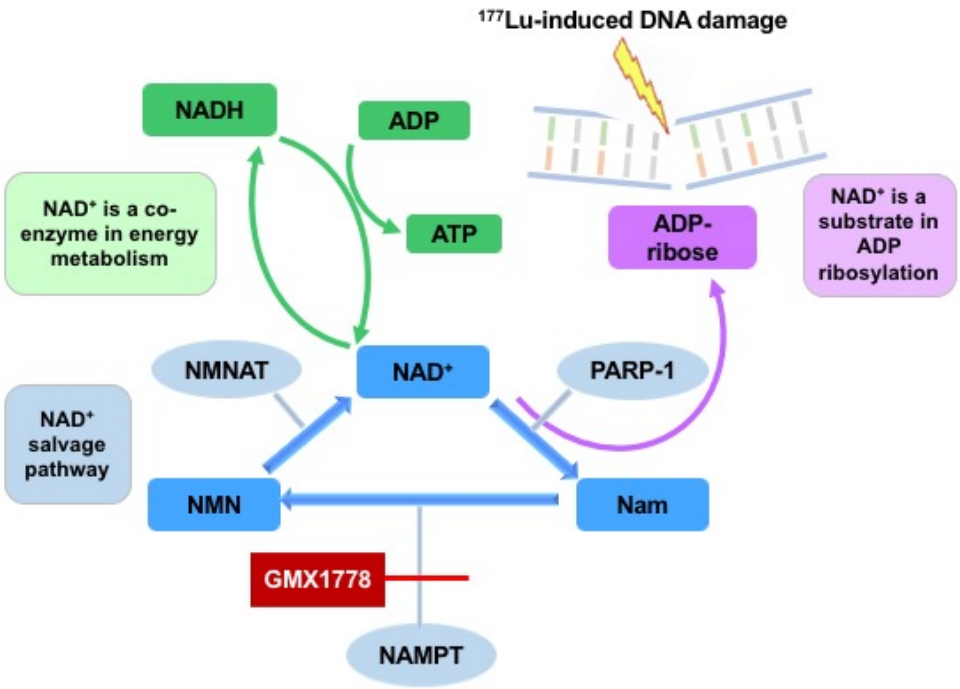

Figure 4. NAD^+ salvage pathway*. Hypothetical model of radiosensitizing effects of NAMPT inhibitor GMX1778. NAMPT inhibition leads to NAD^+ depletion. Since NAD^+ is a co-enzyme in ATP generation, NAD^+ depletion can result in loss of energy stores and thereby cell death. NAD+ = nicotinamide adenine dinucleotide, Nam = nicotinamide, NMN = nicotinamide mononucleotide, NAMPT = Nicotinamide phosphoribosyl transferase, NMNAT = NMN adenyl transferase, PARP = poly(ADP-ribose) polymerase. Adapted from Watson et al. (98).*

Radiosensitization

PRRT of NET is usually administered as a monotherapy in a palliative setting, the dose chosen to avoid severe side effects. However, the efficacy of treatment can be modulated by either making the tumour cells more radiosensitive (radiosensitization) or the normal tissues less radiosensitive (radioprotection), and thereby widening the therapeutic window of PRRT. As previously described, parallel infusions of amino acids are given for radioprotective reasons. As a way of increasing the tumoricidal effect, PRRT has been combined with chemotherapy (101-104). Though in a true meaning, a radiosensitizer has a mechanism of action that is synergistic with the cytotoxic radiation and is relatively nontoxic in itself, acting only to potentiate the radiation toxicity.

EVALUATION OF TREATMENT RESPONSE

The evaluation of treatment is based on symptoms, biochemistry and morphology. In SI-NETs, symptomatic improvement can be measured as less frequency of diarrhoea or flushing episodes. Biochemical tumour markers are often monitored and the levels are supposedly reflecting the volume of remaining tumour tissue (105). A decrease in chromogranin A (CgA) has in some studies been suggested as a predictive marker for morphological response (106), while others claim the opposite (107). Further, there are several pitfalls when using biomarkers as treatment response evaluation (108, 109). Use of proton pump inhibitors elevate both chromogranin A and gastrin, and several foods and drugs affect the level of 5-HIAA in urine. Hence, awareness and caution must be used when interpreting biomarkers.

Imaging modalities, *e.g.* CT and MRI, are possibly more objective and repeatable evaluative instruments.

RECIST criteria

Cross-sectional morphological imaging by CT and MRI is the mainstay for surveillance and detection of recurrent disease in NETs. The tumour extent is quantified by measuring the diameter of the tumour lesions. This is clinically easily applied and there are different guidelines or rules on how to interpret the radiological findings. A widely accepted set of rules is the RECIST criteria (110). In RECIST, target lesions are identified in the obtained images. These are tumour lesions with a diameter of at least 10 mm, or a lymph node tumour

where the short axis measures at least 15 mm. Bone lesions are not regarded as target lesions and can thus not be used. All measurable lesions up to 10 lesions in total (maximum 5 organs, up to 2 lesions per organ) are recorded. The sum of their longest diameter (LD) is then used in evaluation of treatment response. Target lesions should also be selected for their suitability for accurate repeated measurements, *i.e.* all lesions should be assessable in all images used. Size change of tumour lesions is then established as:

Complete Response (CR): Disappearance of all target lesions

Partial Response (PR): At least a 30% decrease in the sum of the LD of target lesions, compared to the baseline sum LD

Progressive Disease (PD): The appearance of one or more new lesions or at least a 20% increase in the sum of the LD of target lesions, compared to the smallest sum LD recorded since the treatment started

Stable Disease (SD): Neither sufficient shrinkage to qualify for PR nor sufficient increase to qualify for PD, taking as reference the smallest sum LD since the treatment started

---

CR and PR are together often referred to as objective response. This assessment of treatment response is simple and robust, but demands a substantial tumour shrinkage to show an objective response. Treatments can result in necrosis and swelling, thus no decreased tumour size can be detected. Also, NETs are generally slow-growing and it can take a long time to detect a change in tumour size. Therefore, it has been debated whether this morphological evaluation is appropriate for assessment of NETs (111, 112).

Diffusion weighted imaging

Diffusion weighted imaging (DWI) is a functional technique applied in MRI. It visualizes changes in diffusion of water molecules in tissue, reflecting the micro-environment (111, 113). The change in diffusion can be detected after anti-tumoral treatment, which leads to oedema in the tumour and disruption of cell membranes. This affects the ability for water molecules to move freely intra- and extracellularly, *i.e.* diffusion (Fig. 5).

The amount of diffusion-sensitization applied is indicated by the b-value, which is dependent in a specific mathematical way on the magnetic gradient amplitude, the duration of the gradient and the time between the two gradients applied in the sequence. The higher the b-value, the more sensitive an image is to the effect of diffusion. The diffusion can be quantified in a more precise way by the apparent diffusion coefficient (ADC). ADC is calculated by performing imaging using two or more b-values. At high b-values (> 100 s/mm^2) the signal attenuation primarily depends on molecular diffusion, while at low b-values (< 100 s/mm^2) perfusion (capillary blood flow) leads to additional signal attenuation. This means that $ADC_{(0\text{-}800)}$ is sensitive to diffusion as well as to microperfusion, while $ADC_{(120\text{-}800)}$ is sensitive to diffusion exclusively.

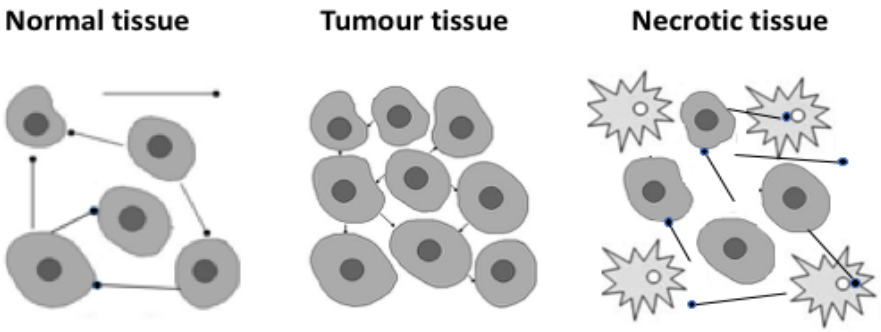

Figure 5. Diffusion in the cellular microenvironment. *Diffusion, depicted by lines, varies depending on cell density, amount of extra-cellular space and the integrity of cellular membranes. Illustration by V. Johanson*

Studies on tumour response evaluation with DWI have demonstrated that a functional response is often earlier detectable than an anatomical (46, 114). Theoretically the initial treatment response affects tumour viability rather than size (115). Post-treatment evaluation with DWI has also been studied in NETs (116-118).

There are currently no uniform protocols on how to assess NET treatment response with DWI, but this functional method seems to be an important new tool for tumour evaluation (118-120).

Dosimetry of ^{177}Lu-DOTATATE

Dosimetry is the way to measure the absorbed dose in tissue, which is used to predict and determine the effects of radiation. The absorbed dose is defined as the amount of energy deposited in a tissue by radiation per unit mass of the tissue and has the unit Gray (Gy = Joule/kg). When using gamma-emitting radionuclides, the radiation can be detected and quantified by a gamma camera with planar or SPECT imaging (Fig. 6). After the radionuclide injection, a biokinetic estimation of the decay in tissue is performed by repeated imaging, enabling the calculation of the cumulative activity (121). Frequent imaging is needed to make as precise estimates of the uptake and elimination of the activity as possible, and both early and late time points are necessary to capture the dynamics.

Calculation of the cumulative activity of the radiopharmaceutical is complicated, especially in tumours located in the liver, since the tumours are sometimes small and the normal liver tissue has a physiological uptake of activity. When using planar images, the conjugate view method is the most commonly used model to quantify the activity (122). In planar gamma camera images, a region of interest (ROI) is drawn around the organ or tumour to be measured. The counts recorded are corrected for background counts, using a background ROI located in close proximity (123, 124).

After acquisition of the activity at the different time points, a time-activity curve can be fitted and the accumulated activity is calculated from the area under the curve. In a low-resolution CT the volume of the organ or tumour is estimated. The total electron energy emitted per decay of the radionuclide is obtained, and thereby the absorbed dose can be calculated (125). SPECT imaging at one time point (usually at 24h) can be used as a complement to planar images. The activity of the measured organ or tumour is then obtained directly, and the time-activity curve is adjusted accordingly for a correct activity concentration estimation (126). Calculation of the activity can also be performed by using exclusively SPECT imaging (127).

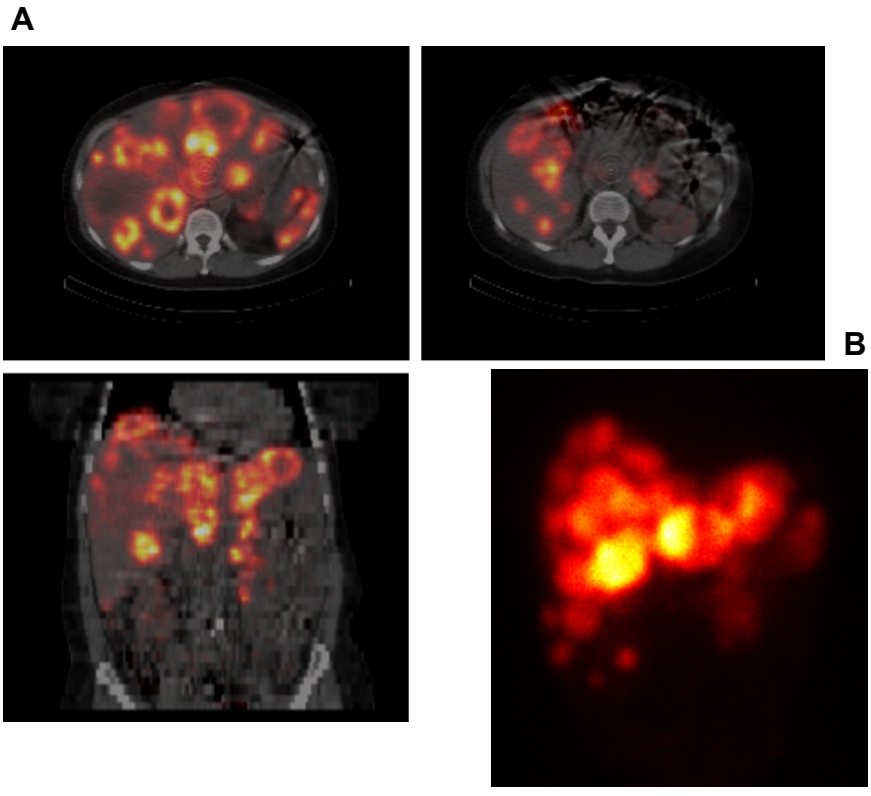

Figure 6. SPECT/CT (A) and anterior-posterior planar (B) images after ^{177}Lu-DOTATATE treatment. *Target lesions from diagnostic CT images are identified and regions of interest are drawn around the lesions, after which activity counts are recorded. When using planar images, the background activity is subtracted to obtain the activity of the lesion.*

Dosimetry of ^{90}Yttrium

There are two different microspheres used for ^{90}Y radioembolization: resin and glass. The spheres differ size and activity amount, which leads to that the treatment volumes differ and thereby the embolic effect (128). The resin spheres are the most commonly used and approximately 50 million spheres are delivered when the whole liver is treated.

Before administration an individual dosimetry is performed. There are three methods to calculate the correct treatment activity and the most frequently used is the Body Surface Area (BSA) method, which relies on empiric data and mainly takes the patient size into account. A somewhat more sophisticated method is the partition model, where a specific equation is used, which regards the tumour/normal tissue ratio of the liver and the decided maximum dose to the normal liver tissue. Also, the lung shunting component is considered, using the preceding scintigraphy with ^{99m}Tc labelled macro-aggregated albumin (^{99m}TcMAA). If the shunting fraction is 10-20% the planned dose is adjusted, and if it exceeds 20%, treatment is not an option due to too high risks for side effects. The partition model is considered to be a better option for dosimetry, since it more reliably avoids exposing the normal tissue for high doses of radiation, which could induce radiotoxic side effects, *e.g.* radiation pneumonitis, radiation induced liver disease (RILD) and radiation ulcer (129).

After the treatment, the biodistribution of the microspheres is verified by imaging. Despite that ^{90}Y is a pure ß emitter, gamma camera measurements can be done. The emitted ß particles generate Bremsstrahlung (photons) and due to the high activity concentration in the liver these can be detected by a gamma camera (130). The activity distribution is therefore visualized by a SPECT after treatment (Fig. 7A). However, depending on the physical characteristics of Bremsstrahlung, the images can be of poor quality, why they are often complemented with a PET (Fig. 7B). This is possible due to a combination of the occasional positron emission in ^{90}Y decay and the relatively high concentration of radioactivity in radioembolization (131).

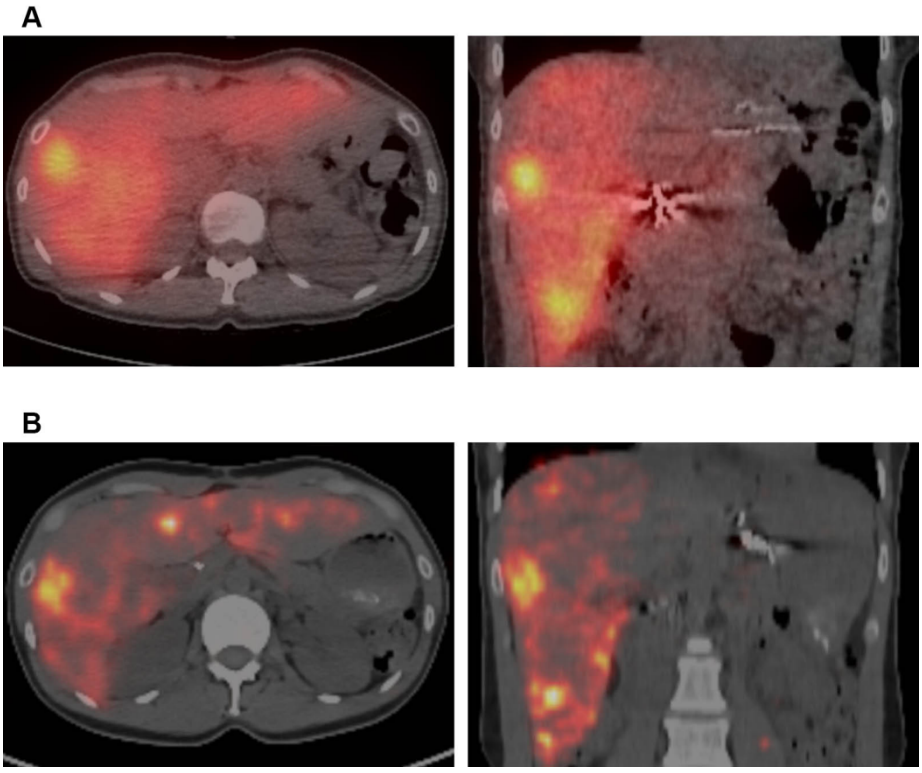

Figure 7. Imaging after ^{90}Y radioembolization, transaxial (left) and coronary (right) views. A) *Bremsstrahlung imaging with SPECT/CT, showing the selective activity uptake in the liver.* ***B)*** *PET/CT images give higher resolution. The yellow areas depict tumour tissue.*

AIMS OF THE THESIS

The use of targeted radionuclide therapy in metastasized NET has increased during the last decade. Treatments are resource demanding and costly with potentially toxic side effects and a highly variable treatment response. The general aims of the thesis were therefore to contribute to a better understanding of treatment with ^{177}Lu-DOTATATE and ^{90}Y hepatic microspheres and thereby improve selection of patients who would benefit from these treatments.

Specific aims were

- To identify prognostic factors for long-term outcome and toxicity, from a consecutive patient series treated with ^{177}Lu-DOTATATE
- To investigate if the absorbed tumour dose at ^{177}Lu-DOTATATE treatment can predict tumour shrinkage
- To investigate if the immunohistochemical expression of SSTR2 can predict outcome after PRRT
- To explore the radiosensitizing effect of the NAMPT inhibitor GMX1778 in SI-NETs
- To compare treatment response and toxicity of hepatic artery embolization (HAE) and radioembolization (RE) in SI-NETs
- To investigate if DWI-MRI can be an early predictor of treatment response after embolization of SI-NET hepatic metastases

MATERIALS AND METHODS

PAPER I - STUDY DESIGN AND PATIENTS

This is a clinical retrospective study on all patients treated with ^{177}Lu-DOTATATE at Sahlgrenska University hospital, Gothenburg, since the treatment was initiated in 2006 until 2011. All patients had tumours with an uptake on somatostatin scintigraphy (Octreoscan®) exceeding physiological liver uptake. Patient characteristics and indication for treatment are shown in Table 3.

Biochemical response and radiological response according to RECIST 1.1 (110) were analysed. Best morphological response (BR) was also calculated on a lesion-by-lesion basis. To calculate BR the relative change in longest diameter of each tumour, from baseline until the time of the smallest measurement of the same diameter, was analysed.

Long-term treatment outcome including progression-free survival (PFS) and overall survival (OS) was obtained. Long-term renal and haematological toxicities were evaluated by glomerular filtration rate (GFR) and blood cell count, respectively. Toxicities were graded according to common toxic criteria for adverse events (CTCAE v. 4.0). Renal and tumour dosimetry were performed.

	SI-NET	Pan-NET	Rectal NET	Kidney NET	Presacral carcinoid	Lung carcinoid	Neuroblastoma	**Total**
n	31	11	4	2	1	1	1	**51**
Median age	63	54	65	38	41	64	38	**59**
Male sex	18	5	3	2	1	1	1	**31**
Tumor grade								
1	19	2		2	1			**24**
2	5	7	3					**15**
3		1	1				1	**3**
Not evaluated	7	1				1		**9**
Indication								
Progressive disease	21	8	4	1		1		**35**
Inoperable disease	6	1		1	1		1	**10**
Adjuvant therapy	1							**1**
Neoadjuvant therapy		1						**1**
Excessive symptoms	3	1						**4**

Table 3. Patient, tumour and treatment characteristics. *Tumour grade according to WHO classification (4th edition).*

^{177}Lu-DOTATATE treatment and dosimetry

An average amount of 7.5 GBq (range 3.5 – 8.2 GBq) ^{177}Lu-DOTATATE was given as a 30-min intravenous infusion co-administered with kidney protective amino acids (2.5 % lysine and 2.5 % arginine in 1 L of 0.9 % NaCl) for 4 hours. The treatments were repeated approximately every 8 weeks (range 6 – 10 weeks). All but 3 patients were planned for 4 treatments, but 23 patients discontinued therapy for different reasons: risk of exceeding renal dose limit (*n*=11), persistent haematological toxicity (*n*=5), low performance status (*n*=2), rapid disease progression and death (*n*=4) or own choice (*n*=1). Four patients received 5 treatments.

Planar gamma camera images were obtained at 1.5, 24, 48 and 168 h after ^{177}Lu-DOTATATE treatment. These images, combined with a single photon emission computed tomography and a low-resolution CT (SPECT/CT) at 24 h were used for dosimetry.

Renal dosimetry was performed using the conjugate view method (122). The effective attenuation coefficient, sensitivity, anterior and posterior counts from the planar images were obtained. The counts in the anterior and posterior images in a region of interest (ROI) surrounding the kidney were recorded and the counts in a background ROI located caudal to the kidney ROI were subtracted. Patient and kidney thickness were determined in the CT. A monoexponential curve fit was applied to the time-activity data and the accumulated activity was calculated.

Tumour dosimetry was performed on the target lesions used in the RECIST evaluation. Activity concentration was measured in the SPECT/CT images, which were reconstructed with our recently developed Monte Carlo based ordered subset expectation maximum reconstruction method SARec (132). The background ROI and the tumour ROI were drawn in geometrical mean images of the planar anterior and posterior images. The conjugate view method was applied and a biexponential time-activity curve was fitted and matched to the activity concentration from the SPECT/CT.

The cumulative absorbed dose to the tumours until date of best response (BR) was also calculated. The relationship between the cumulative absorbed dose and BR was evaluated using linear regression analysis.

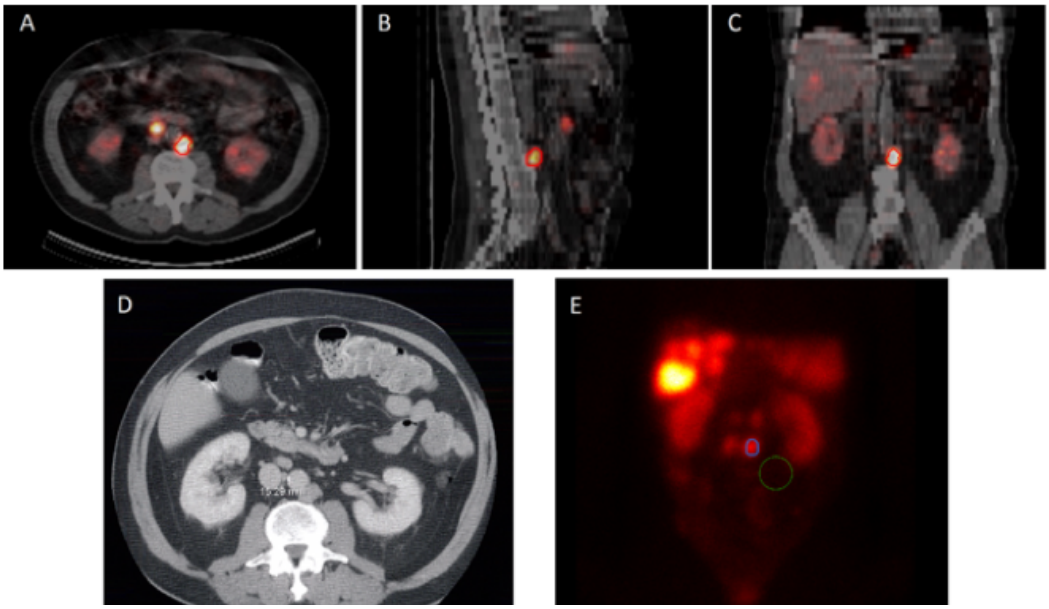

Figure 8. Images used for tumour dosimetry. A-C) *SPECT/CT images where tumour region of interest (ROI) was drawn around para-aortal tumour lesion.* ***D)*** *Diagnostic CT where target lesions were identified.* ***E)*** *Planar images anterior-posterior view, where tumour and background ROIs are indicated.*

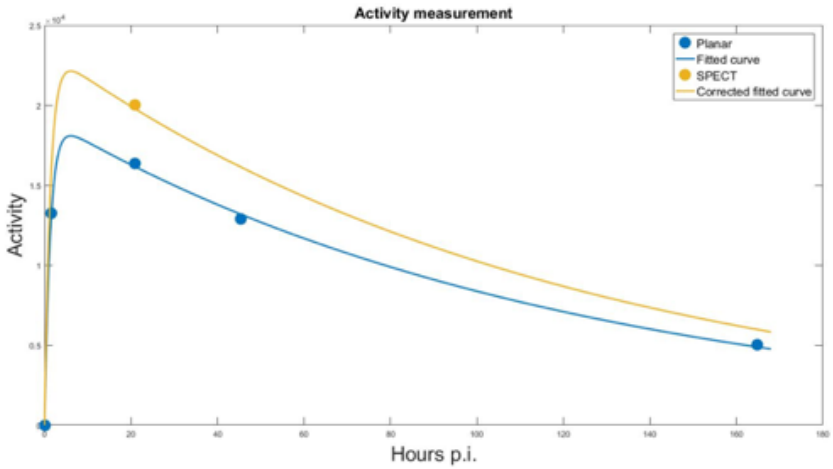

Figure 9. Activity calculation by a biexponential curve fitted from activity measurements in repeated planar and SPECT images. *P.i. = post-injection of PRRT.*

PAPER II – STUDY DESIGN AND PATIENTS

In this study we wanted to explore the relationship between immunohistochemical (IHC) expression of SSTR2 and long-term outcome in ^{177}Lu-DOTATATE treated patients. A previously assembled tissue microarray (TMA) of tumour tissue from 412 patients, who were surgically resected for SI-NET at Sahlgrenska University hospital, Gothenburg during 1986-2013, was used for IHC analysis (133). Two subgroups of patients were identified: Cohort A (*n*=44) included all patients also treated with ^{177}Lu-DOTATATE at SU until 2016 and cohort B (*n*=34) included all patients with specimen from 3 different locations (primary tumour, lymph node and liver metastasis). Cohort B was obtained as a control group for consistency regarding SSTR2 scoring between lesions at different sites. Survival analysis was performed and clinical data regarding treatments was obtained for both cohorts. Two patients in Cohort A (one from each subgroup) were excluded from survival analyses due to that they had rapid disease progression and died before completing PRRT.

Immunohistochemistry and scoring

All TMA blocks were immunohistochemically (IHC) stained for expression of SSTR2, Ki-67, chromogranin A and synaptophysin. Antibodies used were: anti-SSTR2a (clone UMB1; cat no. 134152 [Abcam]), anti-chromogranin A (MAB319; Chemicon), anti-synaptophysin (SY38, M0776; Dako) and anti-Ki67 (MIB1; Dako).

SSTR2 expression was scored semi-quantitatively into one of 4 categories (0-3), depending on level of expression (Fig. 10). The scoring system was based on the immunoreactive scoring method previously described by Specht et al (134). Briefly, using all specimen on the TMA blocks, a score for staining intensity between 0-3 was determined. A scoring (0-4) for percentage stained cells was also performed. These two scores were then multiplied for a combined score of 0-12, which was then divided into separate groups (score 0-1 = group 0, score 2-3= group 1, score 4-8= group 2 and score 9-12 = group 3. When we applied this method to cohort A and B samples a consistently homogenous expression pattern was found, with over 80% stained cells in all samples with the exception of 4 negative samples (*i.e.* score 0). Therefore, staining intensity was the primary determinant for final score.

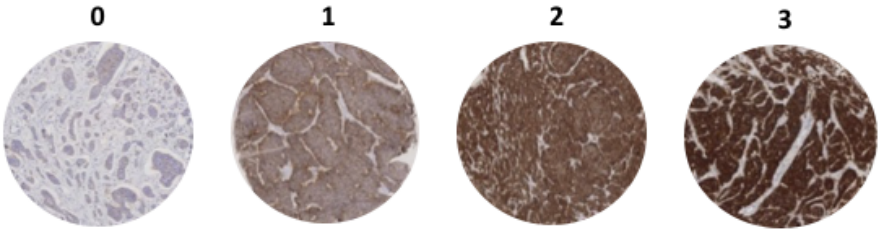

Figure 10. SSTR2 scoring. *Homogenous expression pattern of cells, therefore staining intensity was the determinant for SSTR2 score.*

Activity concentration in tumours

In ^{177}Lu-DOTATATE treated patients (cohort A) an estimation of the uptake of radionuclide was done by measuring the activity concentration in SPECT images, obtained 24h after treatment. Tumours were identified by visual inspection of images, and up to 3 tumours containing the highest maximum voxel values in each patient were chosen for assessment. Activity concentration calculation was done by dividing the maximum voxel value with SPECT sensitivity and mass of the tissue represented by the voxel. Then, the activity was divides by the amount of injected activity, giving the specific activity concentration.

PAPER III – SUBJECTS AND METHODS

Paper III is an experimental study on female BALB/c nude mice xenografted with tumours derived from the cell line GOT1, which is a human SI-NET cell line. The xenografting procedure is previously described (135). Tumour-bearing animals were divided into 6 treatment groups (Table 4).

Group	Treatment
1 (*n*=6)	Controls
2 (*n*=10)	^{177}Lu-DOTATATE (7.5 MBq)
3 (*n*=7)	GMX1778 x 1 (100mg/kg)
4 (*n*=5)	GMX1778 x 3 (3 weekly doses of 100mg/kg)
5 (*n*=6)	^{177}Lu-DOTATATE (7.5 MBq) + GMX1778 x 1 (100mg/kg)
6 (*n*=5)	^{177}Lu-DOTATATE (7.5 MBq) + GMX1778 x 3 (100mg/kg/w)

Table 4. *Groups and treatments in study III.*

^{177}Lu-DOTATATE, with a specific activity of 30MBq/µg, was administered by injection into the tail vein.

GMX1778 (N-(6-chlorophenoxyhexyl)-N'-cyano-N''-4-pyridylguanidine) was formulated as a 20mg/mL suspension in 2% carboxymethyl cellulose in 0.9% saline. The drug was administered by oral gavage either as single dose or repeated weekly for 3 doses. In the groups with combined therapy, GMX1778 was given 1h after ^{177}Lu-DOTATATE.

The animals were monitored regularly with measurements of weight and tumour size. Tumour volumes were calculated by assuming spheroid shapes ($V = 4\pi r_1\, r_2\, r_3\, /\, 3$). The animals were followed up to 17 weeks and killed when tumour weight exceeded 10% of body weight or if body weight decreased more than 10%.

For biochemical evaluation of NAD^+, *in vitro* studies were performed. GOT1 cells were cultured as previously described (99) and divided into 4 treatment groups (Table 5). After incubation for 1h with GMX1778 at 10 or 0 nM, cells were irradiated with 1 or 0 Gy. Cells were harvested at 1, 5 and 14h after irradiation. Cells were pelleted and analysed for NAD^+ by liquid chromatography-mass spectrometry.

Group	Treatment
1	control
2	GMX1778 (10 nM)
3	external irradiation (1 Gy)
4	GMX1778 (10 nM) + external radiation (1 Gy)

Table 5. *Treatment groups in cultured GOT1 cells.*

PAPER IV – PATIENTS AND METHODS

This is a prospective study on patients with multiple hepatic SI-NET metastases not accessible to curative resection or ablation. All patients had previous resection of all extra-hepatic tumours and were then randomized to either hepatic artery embolization (HAE) or radioembolization (RE) with ^{90}Y-microspheres. Radiological and biochemical tumour marker evaluations were performed. Haematological and liver-specific toxicity was monitored weekly

during the first month and after 3 and 6 months. Patient and tumour characteristics in Table 6.

Embolization procedures

The work-up preceding radioembolization (RE) included angiography with protective coiling of the gastroduodenal artery and determination of shunting between liver and lung circulation via scintigraphy with ^{99m}Tc-MAA in a standardized manner (136). RE was performed by depositing ^{90}Y resin microspheres (SIR-spheres®, delivered by SIRTex) (diameter 20-60 μm) in the common hepatic artery with activity calculation using the partition model (129).

Hepatic artery embolization (HAE) was performed using polyvinyl alcohol particles (diameter 45-150 μm) into the right or left hepatic artery until stasis was achieved. The right lobe was embolized first, repeating the procedure in the left lobe after median 6 (range 5-10) weeks.

Imaging and analysis

Magnetic resonance imaging (MRI) including T1 and T2 weighted scans and diffusion weighted imaging (DWI) scan with multiple *b*-values were performed at baseline and 1, 3 and 6 months after treatment. A T1-weighted dynamic contrast-enhanced sequence in late arterial and portal venous phases was added in examinations at baseline, 3 and 6 months.

Up to 5 liver metastases were analysed per patient. Multiple regions of interest (ROI) were drawn around the tumours to include the whole tumour volume on the DWI images. The relative ADC values were calculated and data from baseline and 1-month images were used for comparison.

Response evaluation was performed according to RECIST 1.1 (Eisenhauer 2009) using the two best measurable and representative lesions in each patient. The response was also determined on a lesion-by-lesion basis, by calculating the change in the longest diameter (LD) in all assessable tumours.

	All patients (n= 11)	RE treatment (n= 6)	HAE treatment (n=5)
Age, years, median (range)	67 (40-79)	66.5 (40-79)	67 (51-79)
Male sex (%)	3 (27)	2 (33)	1 (20)
Number of lesions analysed, median (range)	4 (1-5)	5 (2-5)	3 (1-5)
Median LD, mm (range)	20.3 (13-55)	20.3 (13-50)	19.9 (13-55)
Median sum of LD of metastases analysed, mm (range)	77 (30-170)	89 (35-170)	74 (30-170)
Median baseline $ADC_{(120-800)}$, $10^{-3}mm^2/s$ (range)	0.73 (0.5-1.3)	0.78 (0.5-1.3)	0.68 (0.5-1.0)
Primary tumour, grade 1 (Ki-67 <3%) (*n*)	7	5	2
Primary tumour, grade 2 (Ki-67 3-20%) (*n*)	4	1	3
Median dU-5HIAA (µmol/24h) (range)	110 (21-270)	97 (54-130)	110 (21-270)
Median S-CgA (µg/L) (range)	231 (81-1890)	162 (81-470)	384 (115-1890)

Table 6. Baseline clinical and tumour characteristics. *RE = radioembolization, HAE = hepatic artery embolization, LD = longest diameter, ADC = apparent diffusion coefficient, dU-5HIAA and CgA = tumour biomarkers.*

ETHICAL CONSIDERATIONS

Studies I, II and IV were approved by the Regional Medical Ethics Committee in Gothenburg. Diary numbers are 833-12, 373-05 and 540-13, respectively.

Study III was approved by the Ethical Committee for animal research at the University of Gothenburg. Diary number 341-2005.

STATISTICS

Kaplan Meier curves were used for PFS and OS in study I-II and for time to tumour progression in study III. Mantel-Cox log-rank test was used for comparison of curves.

For dosimetry relationships in paper I t-test and linear regression were used. For all statistical analyses of data generated from IHC scoring in paper II, non-parametric tests were used. For comparisons between two groups Mann-Whitney U test was used. For comparisons between 3 or more groups Kruskal-Wallis one-way ANOVA was used. Tukey's multiple comparison was applied when needed for correction of *p* values. Prizm software (version 7.0) and Excel (version 16.15) were used for statistical analyses.

In paper IV radiological response rates were estimated by binomial proportions and compared with Fischer´s exact test, using MedCalc statistics package (MedCalc Software, Ostend, Belgium). Linear mixed models were used to test for difference between changes in ADC parameters and for linear correlation between ADC parameters and change in tumour size. These calculations were performed in MATLAB 2016b (MathWorks Inc, Natick, MA, USA). Mann-Whitney *U* test or Wilcoxon signed-rank test were used for comparing differences in continuous variables.

In all tests a p value of <0.05 was considered statistically significant.

RESULTS

RETROSPECTIVE STUDY OF ^{177}LU-DOTATATE

Fifty-one patients received ^{177}Lu-DOTATATE treatment from 2006 to 2011, of which 40 were assessable according to RECIST 1.1. Most patients (n = 33; 83%) had stable disease (SD) as the best response after therapy. One patient had CR and 4 had PR, adding up to an objective response rate (CR and PR) of 13%. Progressive disease (PD) was radiologically verified in 2 patients. Subgroup analyses according to diagnoses and tumour grades were performed (Fig. 11). The patients with objective response were predominantly found in pan-NET and non-SI-NET/non-pan-NET group, while SI-NET patients were more likely to have SD as the best response. Patients with G2 tumours were objective responders to a larger extent than patients with G1 and G3 tumours.

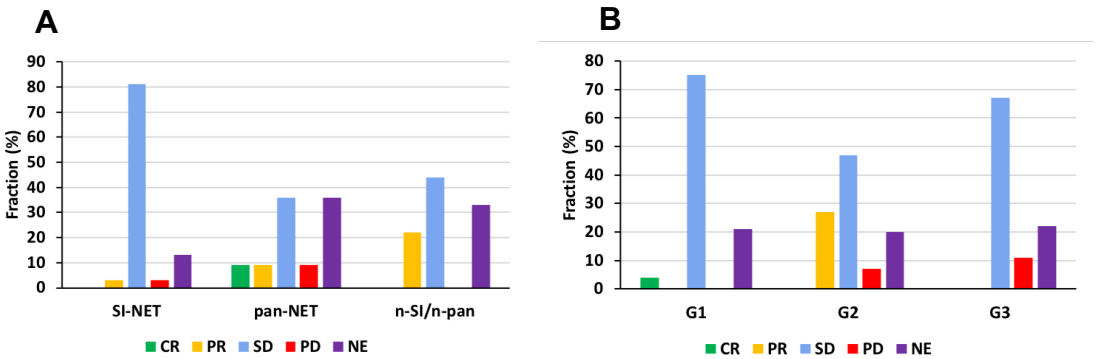

Figure 11. Radiological (RECIST) response per diagnosis (A) and tumour grade (B) after ^{177}Lu-DOTATATE. *Objective responders were mainly found in pan-NET, non-SI-NET/non-pan-NET and G2 subgroups. Results are shown as fractions within subgroup. SI-NET=small intestinal NET, pan-NET=pancreatic NET, n-SI/n-pan=non-SI-NET/non-pan-NET. CR=complete regression, PR=partial regression, SD=stable disease, PD=progressive disease, NE=not evaluated.*

Biochemical response could be analysed in 45 patients, revealing an objective response (≥50% decrease of, or normalized CgA / 24h U-5HIAA) in 33% (n=15) patients. In 18 patients (40%) the tumour markers were changed less than 50%, and 8 of the patients did not have elevated levels of tumour markers at baseline. Four patients had >50% increased biomarkers despite treatment.

Both biochemical and tumour size evaluations were performed in 18 patients, however there was no correlation between these variables (*p=0.51*).

Tumour dosimetry and response

In previously selected RECIST target lesions, tumour dosimetry was performed. This was possible in 24 patients, who had 1-4 tumours assessable in all series of planar scintigraphy and SPECT/CT imaging. Hence, in 52 tumours the absorbed dose was calculated. The median cumulative absorbed dose and specific absorbed dose were 57 Gy (range 10-201) and 2.1 mGy/MBq range 0.39-7.5), respectively, however large inter- and intra-patient variability was observed (Fig. 12).

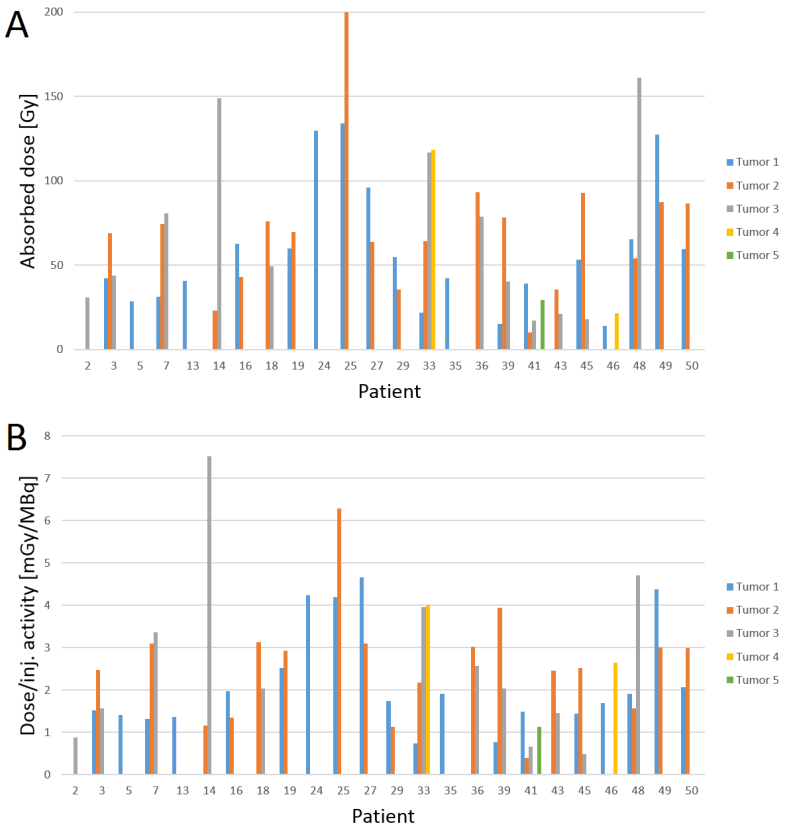

Figure 12. Cumulative absorbed tumour doses and specific absorbed tumour doses in 52 tumours in 24 patients. *Large inter- and intra-patient variability was observed. Gy = Gray, Bq = Bequerel.*

When the relationship between the absorbed tumour dose and the tumour size change was investigated, the tumours from one patient were not assessable in the diagnostic CT images. This resulted in that analyses were possible for 50 tumours in 23 patients. A statistically significant correlation was found between the median absorbed tumour dose and median tumour (*p=0.048*) (Fig.13).

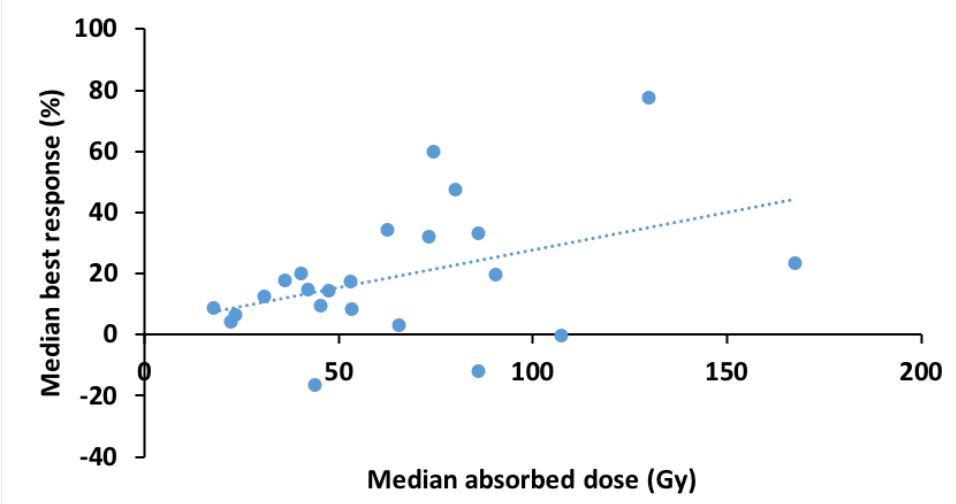

Figure 13. Dose-response curve between median absorbed tumour dose and median best response (tumour diameter shrinkage) in 23 patients. *R=0.42, p=0.048.*

Renal dosimetry and treatments

Calculation of absorbed renal dose was performed after each treatment to avoid exceeding the cumulative kidney dose limit, which was set to 27 Gy. This resulted in reduced doses or cancellation of further treatments for 13 patients. Initially, for calculation of absorbed renal dose, an estimation of the kidney size was performed assuming the shape of an ellipsoid. A later reassessment for a more correct kidney size estimation, using kidney segmentation in the diagnostic CT images, resulted in generally larger kidney sizes and thus lower absorbed renal doses.

The median cumulative absorbed renal dose was 14.4 Gy (range 4-25.9). The relatively low cumulative dose admitted further treatments when the patients

had tumour progression. Ten patients received additional PRRT after 1.5 to 5 years, resulting in a median cumulative absorbed renal dose of 25.8 Gy (range 16.8-44.3) for these patients.

Long-term outcome

The patients were followed for 1-127 (median 65) months. Tumour progression was determined by radiology or by clinical deterioration. Median progression-free survival (PFS) was 45 months (95% CI 29-65 months). Five patients received the treatment as salvage therapy, but had a rapid tumour progression and died within 10 months (median 2 months). In subgroup analyses, no statistically significant differences were seen between diagnoses ($p = 0.13$), but G3 tumours progressed earlier than G1 and G2 tumours (13, 62 and 45 months, respectively) *($p = 0.0001$)* (Fig 14).

Median overall survival (OS) was 51 months for all patients (95% CI 37-69 months). OS was not significantly different between SI-NETs, pan-NETs and other tumours (64, 44 and 86 months, respectively) ($p = 0.99$), but patients with G3 tumours had significantly shorter OS than those with G1 and G2 tumours (18, 74 and 72 months, respectively) *($p = 0.0002$)* (Fig 14).

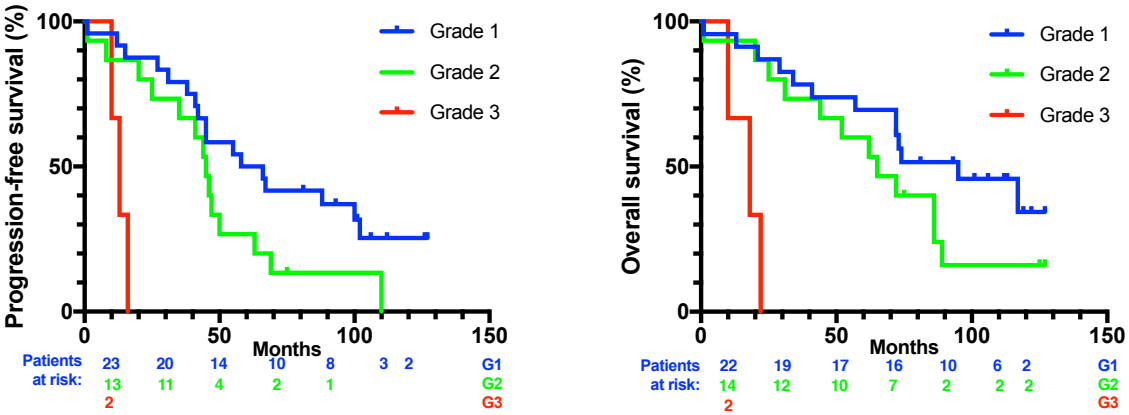

Figure 14. PFS and OS after first ^{177}Lu-DOTATATE. *G3 patients had significantly shorter PFS and OS than G1 and G2 patients (p=0.0001; p=0.0002).*

Toxicity

The median baseline GFR was 78 mL/min/1.73 m^2 (range 44-107) and 5 patients had a GFR below 50 mL/min/1.73 m^2. Evaluation of 30 patients at 17 months (median, range 5-42) after the first treatment showed a GFR decrease of 6.4%. Only one of the patients with low follow-up GFR had a significant decrease from 44 to 29 mL/min/1.73 m^2 after 2 treatments. Long-term GFR was evaluated in 26 patients after median 66 months (range 14-108) after the last treatment, and it had decreased by 16.7% to 64 mL/min/1.73 m^2 (median, range 33-89).

Haematological toxicity was the reason for cancelling planned treatments in 5 patients, who developed grade 3 thrombocytopenia (3 patients) and grade 2 and 3 leukopenia (2 patients). Further one patient, who was previously liver transplanted due to NET hepatic metastases, developed grade 3 thrombocytopenia after the fourth treatment, and had a progressive clinical deterioration and died 8 months after the last treatment. Long-term haematological assessment was performed in 33 patients at 61 months (median; range 11-108) after the last cycle of PRRT. One of the patients who suffered from haematological toxicity had completely recovered after 57 months, but the remaining 4 patients still showed bone marrow impairment.

Nevertheless, despite an advanced tumour stage, most patients could receive all planned treatments without cancellation due to toxicity and no patients developed treatment demanding kidney failure.

SSTR2 EXPRESSION STUDY

For cohort A (PRRT treated patients, $n = 44$), 95 samples were obtained from the tissue microarray (TMA) blocks. The majority of samples ($n = 79$; 83%) had SSTR2 expression scoring 2 or 3. For cohort B (patients with paired samples from primary, lymph node and liver metastases), 102 samples were obtained, among which 79 (77%) had SSTR2 expression scoring 2 or 3. Only 4 samples were completely negative for SSTR2 expression (score 0), and these were all in cohort A.

SSTR2 expression

To determine if the SSTR2 expression was consistent in all lesions within a patient, all samples from metastases in cohort B were sorted according to

SSTR2 expression in corresponding primary tumours. The mean SSTR2 expression was significantly different in metastases from patients with low SSTR2 expression (score 1) in the primary tumour, compared with metastases from primary tumours with higher SSTR2 expression (Fig. 15).

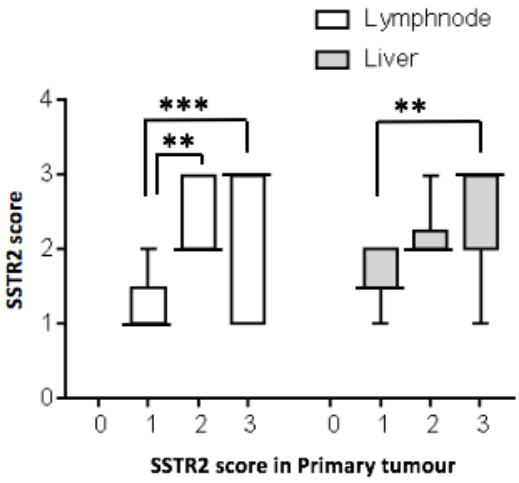

Figure 15. Samples from cohort B sorted according to SSTR2 score in corresponding primary tumour. *A consistency between primary tumours and metastases was observed. SSTR2 expression is significantly different in metastases when sorted according to SSTR2 expression in the primary tumours (**=p< 0.01, ***=p<0.001).Boxes show 25th to 75th percentiles, whiskers indicate ranges and lines show median.*

SSTR2 expression and Ki-67

The patients in cohort A were divided into two groups depending on SSTR expression. Eleven patients had at least one lesion with score 0 or 1 and were assigned to the group "Low SSTR2". The remaining patients ("High SSTR2") (*n*=32) had lesions exclusively scoring 2 or 3. Analysis of tumour proliferation rate revealed a significantly lower Ki-67 among patients with low SSTR2 expressing tumours than in those with high SSTR2 expression *(p=0.048)* (Fig. 16).

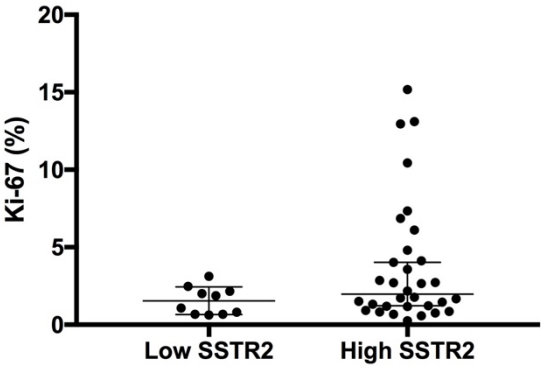

Figure 16. Maximum Ki-67 in patients from cohort A, grouped according to SSTR2 expression. *Patients with high SSTR2 had significantly higher Ki-67 (p=0.048). Bars show median and 95% CI.*

SSTR2 expression and activity concentration

SSTR2 score was also compared with activity concentration in SPECT at 24h after ^{177}Lu-DOTATATE treatment, to estimate the uptake of the radionuclide in the tumours. Up to 3 of the lesions with the highest activities were measured in each patient. There was a large variability between the 33 patients with assessable images (27 with high and 6 with low SSTR2 expressing tumours), and the mean activity was 1.51 and 1.91 MBq/g for the High and Low SSTR2 expressing groups, respectively. Hence, a tendency towards higher activity concentration was observed in patients in Low SSTR2 group, however the difference was not statistically significant *(p = 0.06)* (Fig. 17).

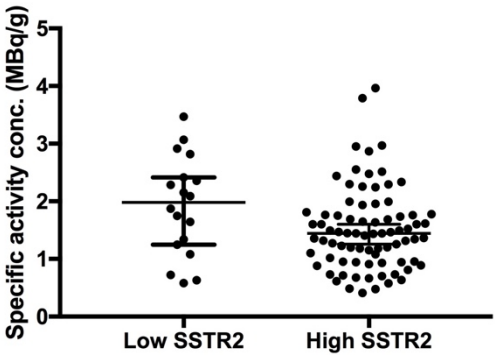

Figure 17. Activity concentration in patients from cohort A grouped according to SSTR2 expression. *Patients in Low SSTR2 group had a tendency towards higher activity concentration, measured in 2-3 lesions in SPECT images at 24h after first ^{177}Lu-DOTATATE treatment (p=0.06). Lines show median and 95% CI.*

SSTR2 expression and long-term outcome

Overall survival (OS) figures were obtained for both cohorts and analysed according to SSTR2 expression. No statistically significant difference between the groups *(p=0.12 for cohort A; p=0.11 for cohort B)* (Fig 18). A trend towards longer survival was seen in the low SSTR2 group in cohort A, which was also strengthened by the complete lack of additional treatment after PRRT in this group *(data not shown)*. In contrast, 25% (*n*=8) of the patients with high SSTR2 expressing tumours received additional treatment for NET after PRRT.

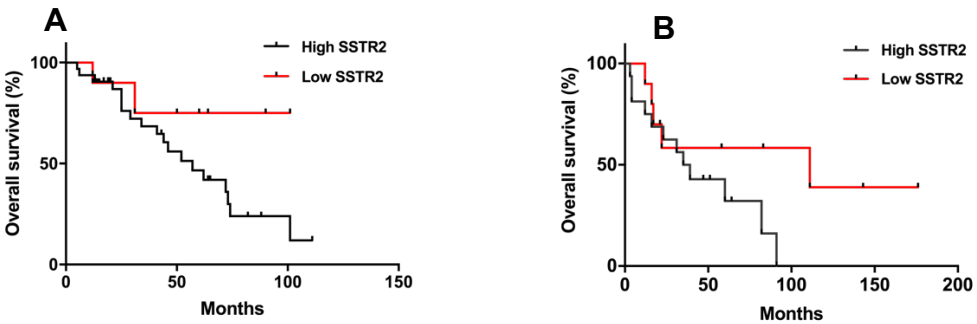

Figure 18. OS in cohorts A (A) and B (B), grouped according to SSTR2 expression*. Cohort A: n=42 (Low SSTR2 n=10; High SSTR2 n=32), cohort B: n=28 (Low SSTR2 n=11; High SSTR2 n=17). A trend towards longer OS was seen for Low SSTR2 groups. in cohort A, however there was no statistical difference between groups (Cohort A: p=0.12; Cohort B: p=0.11).*

RADIOSENSITIZATION STUDY

Treatment with a semi-efficient dose of ^{177}Lu-DOTATATE (7.5 MBq) resulted in mean 45% reduction of tumour volume, compared to baseline. The animals receiving GMX1778 (100mg/kg) in a single or 3 weekly doses had a 34% and 53% mean tumour volume reduction, respectively. When a combination of ^{177}Lu-DOTATATE and single dose GMX1778 was used, the mean tumour reduction was 73% after 3 weeks. Combining ^{177}Lu-DOTATATE and 3 weekly doses of GMX1778 resulted in a mean tumour volume reduction of 97% after 4 weeks, and the tumour in one of the animals was completely eradicated with no signs of tumour recurrence at the end of the study (after 17 weeks) (Fig. 19A).

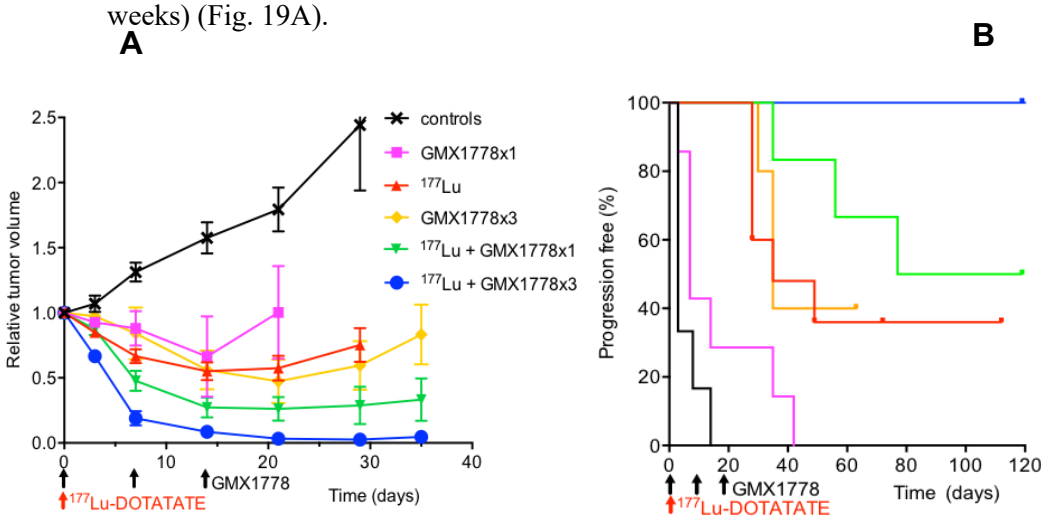

Figure 19. Tumour volume and time to tumour progression of animals. *Treatment with semi-efficient doses PRRT or GMX1778 resulted in modest tumour regression, but combining PRRT with 3 doses GMX1778 resulted in almost eradicated tumours. No tumours in this group progressed, i.e. exceeded volume at the study start. Graph A shows median and bars indicate SEM. Ticks indicate censored data.*

Tumour progression was defined as tumour volume exceeding the volume at the start of the experiment. A single dose of GMX1778 delayed median time to tumour progression marginally (from 3 to 7 days) compared with controls. Treatment with ^{177}Lu-DOTATATE or 3 weekly doses of GMX1778 further delayed the median time to tumour progression to 35 days. In the combination group with ^{177}Lu-DOTATATE and 3 weekly GMX1778 doses 4 of 5 tumours eventually had an increased tumour size but none of them showed tumour progression, *i.e.* exceeded the initial volume (Fig 19B).

Treatment effect on NAD^+ levels

Cultured GOT1 cells were incubated with a low dose of GMX1778 (10 nM) or irradiated with 1 Gy, or a combination of both, or received no treatment. These doses have a slightly cytotoxic effect, not visible until several days after treatment. Irradiation did not affect NAD^+ levels, but in the samples with GMX1778, the amount of NAD^+ was clearly reduced after 5 h and a more pronounced effect was seen after 14 h (Fig. 20). This demonstrates that GMX1778 affects the NAD^+ levels in the tumour cells.

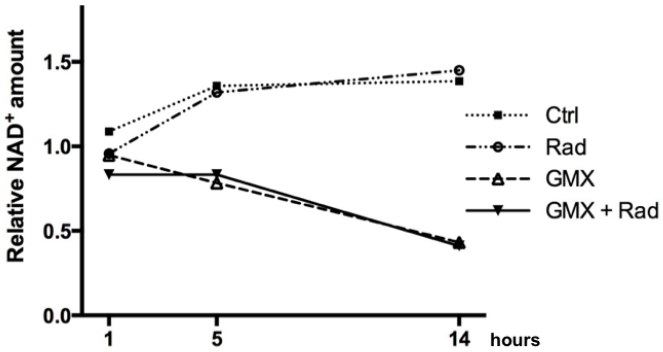

Figure 20. Relative NAD^+ levels in cultured GOT1 cells. *Cells were incubated for up to 14 h with GMX1778 (10 or 0 nM) and were irradiated with 1 or 0 Gy at the start of incubation. NAD^+ levels decreased distinctly in cells treated with GMX1778.*

STUDY ON TREATMENT OF HEPATIC METASTASES

Six patients with SI-NET hepatic metastases were randomized to radioembolization (RE) and 5 to hepatic artery embolization (HAE). One patient could not undergo MRI due to a cardiac pacemaker, and was therefore assigned to CT examinations.

According to RECIST1.1, all of the HAE treated and none of the RE treated patients had PR at 3 months *(p=0.002)*, however all lesions decreased in size. At 6 months one of the HAE treated patients had tumour progression and two of the RE treated patients had PR, which made the difference between the treatment groups statistically insignificant *(p=0.24)* (Fig. 21). In all patients, 39 tumour lesions were assessable on a lesion-by-lesion basis. The decrease of longest diameter (LD) was significantly larger in HAE treated patients than in RE treated patients at both evaluation time points (*p<0.001*).

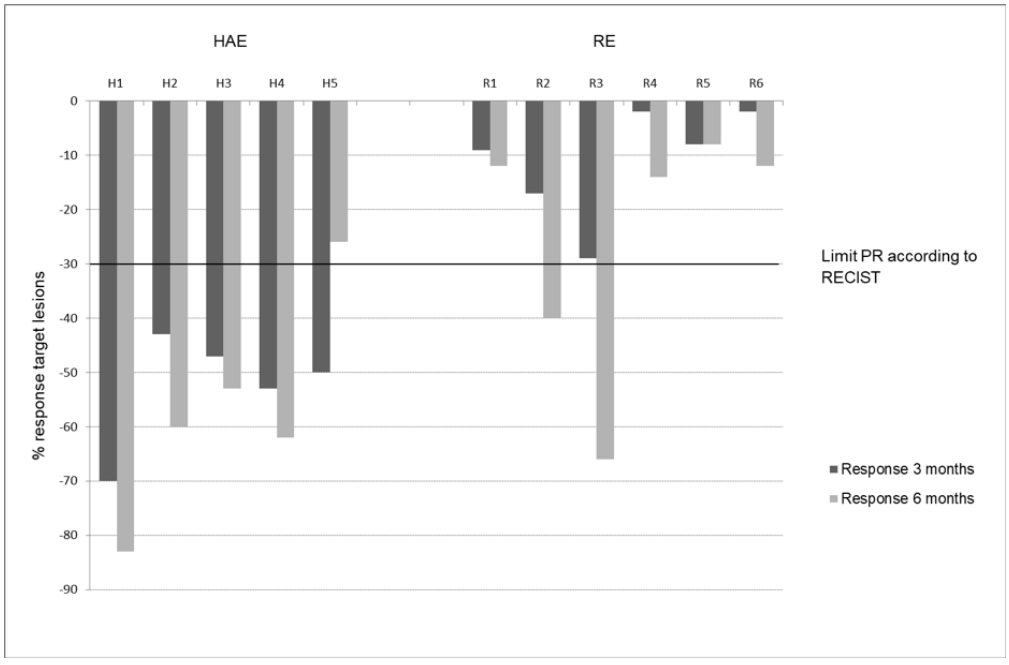

Figure 21. RECIST response at 3 and 6 months in target lesions. *All HAE treated patients and no RE patients had partial response at 3 months, however at 6 months no statistical difference remained between groups. Bars show sum of decrease of 2 tumours in every patient. HAE = hepatic artery embolization, RE = radioembolization.*

Almost all patients had decreased biochemical tumour markers after 3 and 6 months and no difference were seen between treated groups.

Both treatments resulted in low overall toxicity. However, all RE patients but one developed moderately elevated alkaline phosphatase (ALP) levels (median

2.8 µkat/L) after 3 months, which was significantly higher than HAE treated patients (1.4 µkat/L) *(p=0.03)*. The levels were persistent at 6 months. Median hospital stay after HAE was 4 days (range 4-10), which was significantly longer than after RE (2 days, range 2-6).

DWI and treatment response

Ten patients with totally 36 tumours were examined with MRI and diffusion weighted imaging (DWI). The baseline $ADC_{(120\text{-}800)}$ values were significantly negatively correlated with decrease of LD at 6 months, *i.e.* a low baseline $ADC_{(120\text{-}800)}$ was associated with a large tumour shrinkage *(p<0.01)*.

The mean increase of $ADC_{(120\text{-}800)}$ at 1 month after treatment seemed higher in HAE treated patients (40%) compared with RE treated ones (11%), however the difference was not statistically significant (*p=0.08*).

There was a statistically significant correlation between the increase of $ADC_{0\text{-}800}$ at 1 month and the tumour shrinkage at 3 months *(p<0.05)* (Fig. 22).

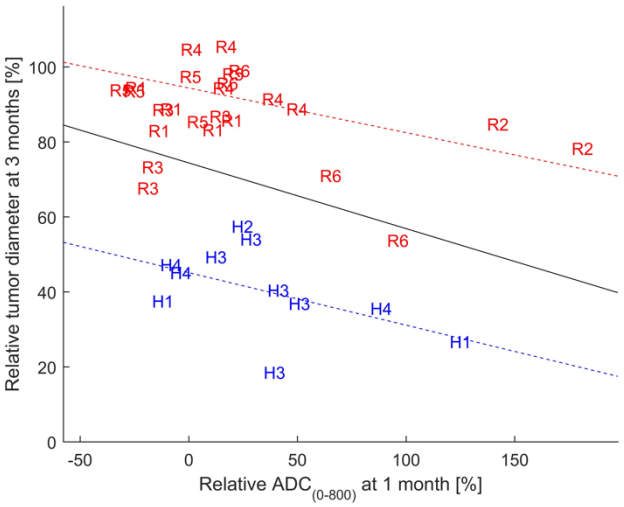

Figure 22. Relative tumour diameter at 3 months of 36 tumours compared with ADC increase at 1 month. *HAE treated tumours were then significantly smaller than RE treated tumours. Blue symbols = hepatic artery embolization (HAE), red symbols = radioembolization (RE). Figures specify patient number.*

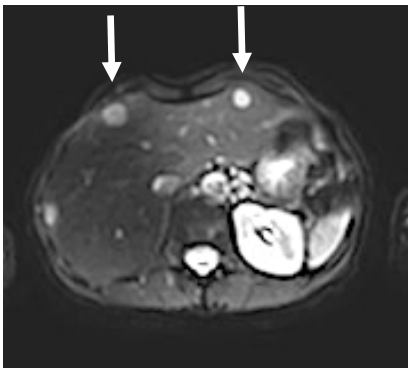

A

Baseline DWI ($ADC_{0\text{-}800}$)

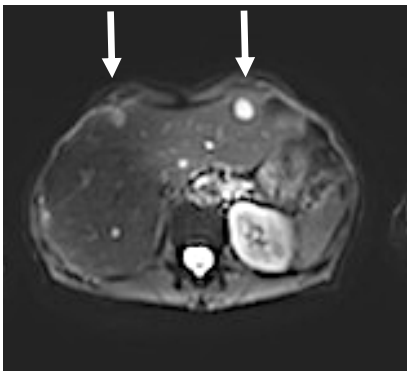

B

DWI ($ADC_{0\text{-}800}$) at 1 month after first HAE

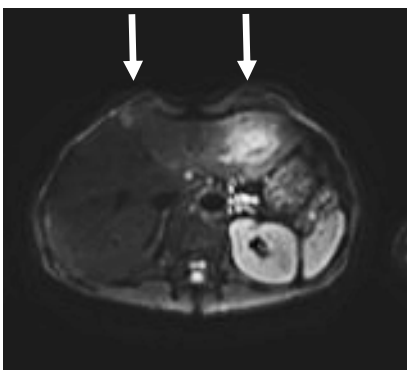

C

DWI ($ADC_{0\text{-}800}$) at 3 months after first HAE

Figure 23. DWI images from third HAE treated patient. *Arrows point at tumour lesions in the left and right lobe, respectively. In baseline image (**A**) the low diffusion of tumours is visualized. In image at 1 month (**B**) the lesion in the right lobe has an increased diffusion, visualized by darker colour, compared with untreated left lesion. Bottom image (**C**) at 3 and 1.5 months after HAE treatment of right and left lobe, respectively. The right tumour is hardly visible, and the area around the left tumour is affected by treatment.*

DISCUSSION

^{177}Lu-DOTATATE and treatment outcome

Among the first 51 patients treated with ^{177}Lu-DOTATATE at Sahlgrenska University hospital 40 patients were evaluated according to RECIST. Twelve per cent of the patients had an objective response (CR + PR). The majority of patients (82%) had SD as the best response which adds up to a disease control rate of 94%. Almost 70% of the patients had progressive disease before treatment, and only 6% (or 14% if including patients with clinical disease progression) after treatment, which should be regarded as a good treatment response. Most patients had slow growing G1 tumours (57%) mainly represented by SI-NET (61% of all patients) but at a disseminated, advanced stage not suitable for alternative treatments, *e.g.* surgery or liver-directed therapy.

Other studies have reported objective response rates higher (76, 83, 84) or lower (137) than in this study, but generally lower proportions of SD. However, it is difficult to make strict comparisons due to sometimes small patient cohorts with heterogeneous NET diagnoses and diverse indications for treatment. In this study, the SI-NET proportion was larger than in other studies (83, 84) and SI-NETs often have a less distinct treatment response (85, 138, 139). SI-NET cells often have a lower proliferation rate than other NETs, *e.g.* pan-NETs, thereby the number of tumour cells susceptible for the DNA damaging effect of PRRT is theoretically fairly low, making them less sensitive to radiation. Hence, this could explain the modest response dynamic after PRRT of SI-NETs.

The median PFS and OS were 45 and 65 months respectively, which is longer than other studies (76, 83, 85, 140). However, PFS and OS was not longer for SI-NET, which is often reported. Obviously, the OS after treatment is affected by the timing of treatment. At the unit for endocrine surgery in Gothenburg, the mainstay for first-line treatment of well-differentiated NET has been surgery performed as radical as possible(141). Repeated surgery was offered for recurring tumours regardless of location, if resectable. Further, patients with liver-dominated disease were often treated with liver-directed therapy, *e.g.* HAE or RF ablation. PRRT was the treatment option exclusively for advanced, unresectable tumours.

Furthermore, the selection of patients is crucial. Present study included a large proportion of G1 and G2 tumours in the lower range, which probably affected the long-term outcome. In subgroup analyses G1 and G2 tumours had significantly longer PFS and OS than G3 tumours, which is well in accordance with the known strong prognostic importance of tumour grade (6). The long median follow-up time (65 months; range 1-127) in our study ensured reliable figures of PFS and OS, hence this avoids too many censored patients in analysis of these slow-growing tumours.

Dosimetry and tumour response

The administered dose of ^{177}Lu-DOTATATE is obviously important for treatment outcome (87). However, the treatment can cause radiotoxic haematological side effects, *e.g.* thrombocytopenia, leukopenia and anemia, and a risk of decreased renal function. These side effects vary inter-individually, and the exact dose limit for a safe treatment is not yet clarified. Previous studies have shown that haematological side effects and absorbed renal dose correlate with pre-treatment renal function (80). However, at low glomerular filtration rates (GFR) the absorbed renal doses vary substantially. Therefore, the absorbed renal dose, and thus the potential renal radiotoxicity, is hard to predict in patients with low GFR (<60 mL/min/1.73 m^2).

In this study the absorbed renal dose limit was set to 27 Gy. Several patients (23%) discontinued treatment due to a risk of exceeding this limit, however after a correction of kidney size the absorbed doses were adjusted. This resulted in a relatively low renal absorbed dose (median 14.4 Gy). In a recently published study a renal dose-driven protocol for treatment with ^{177}Lu-DOTATATE was proposed (85). They demonstrated that an absorbed renal dose exceeding 23 Gy (which is the maximum renal dose limit in several studies) resulted in an increased probability for objective radiological response and prolonged PFS and OS. This seems reasonable, however few studies present data on absorbed tumour dose, *i.e.* the radiotherapy reaching the actual target.

The absorbed tumour dose is an obvious topic to study in relation to examining the efficacy of PRRT, but few studies actually present data on this relationship (127, 142). Tumour dosimetry is demanding, since it includes many parameters to correct for, *e.g.* background, scatter, attenuation and sensitivity of the system (143). Many tumours are located in the liver where the physiological radionuclide uptake can be a disturbance. Also, it is difficult to estimate the correct activity in small tumours due to the partial volume effect. Further, the

activity curve reflecting the biokinetics of the radionuclide is an estimation, since actual measurements at frequent time points are not feasible in the clinic. In this study tumour dosimetry was performed. There were large variations between tumours, even when correcting for the administered activity (specific absorbed tumour dose). This variation could be explained by differences in perfusion or SSTR expression of the tumours, leading to disparities in delivery or uptake of the radiopharmaceutical. Alternatively, the proportion and rate of internalization of the radiopharmaceutical could differ between tumours (144). Nevertheless, a correlation between the median absorbed tumour dose and tumour shrinkage was observed. This indicates a PRRT dose-response relationship for various NETs, detected even with the relatively low doses used in this study. This finding is in accordance with other studies (127, 142), however more research is warranted in this scarcely explored field.

SSTR2 expression and clinical outcome in SI-NETS

In study II the SSTR2 expression in SI-NETs was analysed and only few samples lacked or had a low SSTR2 expression. Patients with low SSTR2 expression in the primary tumour had a significantly lower mean expression in metastases than patients with a high SSTR2 expressing primary tumour. Hence, a low SSTR2 expression in the primary tumour, implies a risk of low SSTR2 expression in the remaining metastases. Therefore, our hypothesis was that the clinical outcome of SSTR based therapy, *e.g.* PRRT, was worse for these patients. Surprisingly, these patients needed less additional therapy after PRRT than high SSTR2 expressing patients. Furthermore, they had a trend for longer OS, even if the difference was not statistically significant. These findings are in contrast to other studies who demonstrated a correlation between high SSTR2 expression and long OS (145-147). However, in some of these studies SSTR2 expression was inversely correlated with Ki-67, and the tumour samples were from various NETs, of which some were G3 tumours. As previously described, Ki-67 is an independent predictor for long-term outcome (13, 83).

SSTR2 expression and SSTR2 imaging

In this study on well differentiated SI-NETs no positive correlation was seen between SSTR2 expression and activity concentration at SPECT 24 h after PRRT. Contrastingly, there was a tendency towards a negative correlation. It is not unreasonable to expect a positive correlation, since the uptake of the

radiopharmaceutical is mediated by SSTR2. Accordingly, a correlation between SSTR2 expression and the uptake on ^{68}Ga-DOTATATE-PET has been demonstrated in several studies (148-150), however the imaging time points differ between the methods, leading to that PET mainly visualizes the binding to SSTR and SPECT reflects the biokinetics, *e.g.* internalization of the radiopeptide. Furthermore, in compared studies both low- and high-proliferative NETs from various origins were included, and a larger proportion of the samples had low or no SSTR2 expression. Our findings are in accordance with a large study of well-differentiated NETs comprising of mainly SI-NET origin, where a correlation between SSTR2 expression and SSTR imaging neither could not be seen (145).

Radiosensitization of SI-NET

Although PRRT is a good treatment option for many patients with metastasized NET it is still considered to be a palliative treatment. Further research and refinements for this treatment modality is thus needed (151, 152). Different strategies for further improvements could include: combination with other antitumoral treatments like anti-angiogenesis therapy, oncogenic pathway inhibitors or chemotherapy, optimization of the radiopharmaceutical (isotope, peptide, chelator) or increasing the dose of the radiolabelled SSA.

The routine kidney protection measures currently used does not reduce the risk of haematological toxicity, but administration of higher doses of PRRT is probably possible for some patients under careful dosimetric surveillance (85).

In most published clinical studies PRRT has been used as a single modality treatment for metastasized NET. However, reports on combination treatment, *e.g.* with chemotherapy, are emerging (104, 153-155). These show promising results with only modestly increased toxicity.

NAMPT has been described as an attractive target in treatment of cancer (98). Due to frequent DNA damages in tumour cells, there is a continuous need for DNA repair in tumour cells. The enzyme PARP-1 plays an important role in ADP-ribosylation, which in turn is involved in several DNA repair mechanisms (97, 156). This leads to an overactivation of PARP-1 in tumour cells, resulting in a high rate of NAD^+ turnover and a need for constant regeneration via the NAD^+ salvage pathway (96). Theoretically, this high dependence on constant NAD^+ regeneration would make the tumour cells more susceptible to NAMPT inhibitors than normal cells (157, 158). It has been used in experimental models as single treatment (159) or in combination with

radiotherapy (100) or a PARP-1 activator (160), but the few phase I studies published did not show any antitumoral effect (161, 162).

In study III we confirmed our previous findings that semi-efficient doses of ^{177}Lu-DOTATATE (7.5 MBq) or GMX1778 (100 mg/kg/w) result in temporary halted tumour growth or moderate regression in nude mice xenografted with the SI-NET cell line GOT1 (87, 99). When combined, the same doses of ^{177}Lu-DOTATATE and GMX1778 enhanced the antitumoral effect considerably, and resulted in complete or near-complete tumour regression in all animals. The mechanism of action of GMX1778 is considered to be inhibition of the enzyme NAMPT in the NAD^+ salvage pathway (98). Our findings in the *in vitro* experiment support this concept, since GMX1778, but not irradiation alone, reduced NAD^+ levels significantly.

Another target in this pathway is PARP-1 and the use of recently developed PARP-I inhibitors has been introduced in several cancer protocols (163). The rationale for this therapy is that inhibition of PARP-1 leads to a decreased repair of radiation-induced single-strand breaks of DNA, yielding an increased tumour cell death. A recently published paper demonstrates potentiation of ^{177}Lu-DOTATATE with a PARP-1 inhibitor in NET cell lines, as an intriguing new way of radiosensitization (164).

Liver-directed therapy

SI-NET patients with stage IV disease often have the main tumour burden located in the liver, where the tumours can become large and bulky and cause the carcinoid syndrome. In these cases, liver-directed therapy is preferred since it spares the rest of the body from side effects, *e.g.* radiotoxicity after PRRT.

The mainstay for treating large, widespread hepatic metastases at our unit has been HAE (165). The treatment has resulted in satisfactory relief of symptoms, tumour regression and possibly prolonged survival for responding patients (49). However, some patients are not responsive to treatment and side effects related to the induced ischemia can sometimes be cumbersome. We started a prospective study with randomization of patients to either HAE or the recently introduced RE, which in retrospective studies has yielded similar results as HAE, but probably less toxicity and higher tolerability.

The results in study IV showed that both treatment groups had similar RECIST response at 6 months, but HAE treated patients responded earlier than RE patients. When analysed lesion-by-lesion, HAE patients had a significantly

larger tumour shrinkage at 6 months than RE patients. These findings illustrate a difference of the treatments: HAE aims for ischemia and necrosis of the metastases. In contrast, the antitumoral effect of RE is radiotoxicity, and radiosensitivity is in general correlated with proliferation rate as cell death from DNA damage often occurs when the cell with damaged DNA enters mitosis. Since the proliferation rate of SI-NETs usually is very low, this can theoretically explain the different response dynamics.

Side effects of both treatments were mild. Apart from one patient who developed cholecystitis after HAE (the only not cholecystectomized patient) no severe complications were noticed. Notedly, 83% of the RE patients developed increased alkaline phosphatase (ALP) levels. These levels were not affecting the patients clinically, and other liver enzymes or bilirubin were not elevated. The raised ALP levels could be explained by mild radiotoxic effects on the normal liver tissue, and has been reported as the most common biochemical toxicity in several reports (166, 167). RILD is a potentially lethal condition predominantly seen in patients with a previous liver dysfunction or damage, *e.g.* cirrhosis, chemotherapy or hepatitis B or C and is triggered by radiotherapy directed against the liver (168, 169). No cases of RILD were seen among the study patients.

Evaluation with diffusion-weighted MRI

In study IV the baseline and 1-month post-treatment DWI images were compared with morphological response using MRI. We demonstrated that the pretherapeutic diffusion coefficient ($ADC_{120\text{-}800}$) correlated significantly with the morphological tumour response (decrease of tumour size) at 6 months. This finding corresponds well with other reports both on NET (116) as well as colorectal and gastric cancer (170, 171). The biological basis for this finding is uncertain, but it has been shown that malignant tumours in general have lower ADC values than benign tumours (172, 173), and in a recent review of the association between pretreatment ADC and Ki-67 in 12 different tumour entities, a negative correlation was shown in most tumour entities including NETs (174).These findings probably reflect the cell density, as it has been found to inversely correlate with ADC (175). Thus, low ADC values seem to correspond with more high-grade tumours, which respond better to chemotherapy and radiotherapy.

The $ADC_{120\text{-}800}$ increased significantly one month after HAE, but not after RE. An increase of ADC is well described in other studies after intra-arterial therapy of hepatic NET metastases (117, 176). The morphological response after RE was delayed compared to HAE, and it is reasonable to believe that this is also the case for ADC changes, although this has not yet been evaluated in this study. Theoretically, the observed diversities could depend on the differences in mechanism of action of the treatments. Supposedly, HAE directly induces ischemia and necrosis, in contrast to RE, where the DNA damaging radiation is delivered over time and thereby resulting in a slower cell death (177). A post-RE inflammatory response with cellular oedema could also be the cause of a hampered ADC increase, as argued in another study (114).

When the relationship between diffusion and morphology after treatment was investigated we found that the ADC increase could not predict the RECIST response, *i.e.* evaluation using only 2 lesions. However, the increase of $ADC_{0\text{-}800}$ correlated with tumour shrinkage, when analysed on a lesion-by-lesion basis, using all 36 lesions. $ADC_{0\text{-}800}$ reflects both the diffusion and pseudo-diffusion (results from capillary circulation), as opposed to $ADC_{120\text{-}800}$, which mainly captures the diffusion.

In conclusion, our study shows that HAE remains a safe treatment option for liver metastases from SI-NET with results comparing very well with the newer RE treatment modality. Further studies are needed to establish the definitive role of RE and the predictive value of DWI-MRI in these tumours.

CONCLUSIONS

- ^{177}Lu-DOTATATE is an effective and tolerable treatment option for various NETs at an advanced stage. High tumour grade, but not tumour origin, was prognostic for inferior long-term outcome.

- Tumour dosimetry is feasible and the absorbed tumour dose seems to correlate with tumour shrinkage after ^{177}Lu-DOTATATE treatment. However, large variations within and between patients were observed.

- A low expression of SSTR2 in SI-NETs was not a negative prognostic factor for long-term outcome after ^{177}Lu-DOTATATE. Neither was low SSTR2 a negative prognostic factor for SI-NET in general (cohort B in study II). Further, a low SSTR2 expression was not associated with an inferior radionuclide uptake, compared with high expressing tumours.

- GMX1778 can be used as a radiosensitizer with low-dose ^{177}Lu-DOTATATE in nude mice, xenotransplanted with human SI-NET. Both tumour shrinkage and time to tumour progression are increased, compared with treatment with only one of the drugs.

- Tumour response occurred earlier after HAE compared to RE in patients with SI-NET hepatic metastases, but at 6 months no significant difference remained. No patients had severe side effects. HAE remains a safe option for treatment of hepatic metastases from SI-NET.

- A low pre-treatment ADC and a high increase of ADC at 1 month correlated with a large tumour shrinkage at 6 months, after embolization treatment of SI-NET hepatic metastases.

FUTURE PERSPECTIVES

This thesis evokes many questions and challenges to proceed with. Our recently closed prospective multicentre study on ^{177}Lu-DOTATATE (ILUMINET, EudraCT 2011-000240-16) with regular CT scans and blood samplings, will give prerequisites for accurate evaluations. These include continued tumour dosimetry and evaluation of its impact on tumour response. In the ILUMINET study tumour progression at inclusion was mandatory, which will facilitate evaluation of tumour response. Also, as many patients seem to tolerate higher absorbed doses of ^{177}Lu-DOTATATE, more treatment fractions have been administered in several cases, yielding interesting dose-response studies to conduct.

The findings regarding SSTR2 expression were surprising and intriguing. Since PRRT is mediated via the SSTRs there should probably exist a connection with the SSTR expression. However, this connection possibly looks different for SI-NETs than for other tumour entities. The next step is to investigate expression of all SSTR subtypes for correlation with anti-tumoral effect and long-term outcome after ^{177}Lu-DOTATATE. Also, the remaining samples on the TMA should contain further low SSTR2 expressing tumours, which will result in a larger material to perform survival analyses in.

GMX1778 is an interesting substance, that experimentally has resulted in positive radiosenstization findings. The hypothesis regarding the place for GMX1778 is risen from the same biological pathway in the cell as PARP inhibitors, which are recently introduced in NET studies (164, 178). But in contrast, the effect of GMX1778 relies on a preserved high level of PARP activation and thereby NAD^+ consumption. Based on our findings, it would be interesting to apply the substance in a clinical setting, which of course is a demanding process.

The prospective study on liver-directed therapies is still recruiting patients, but the collected data is a source for many analyses. Further studies on the DWI data is planned. The findings of an increased ADC after treatment were expected, but there was a difference between HAE and RE. Based on this and the fact that the tumours responded later after RE than HAE, the next step is to visualize the whole post-treatment ADC dynamic using more time points. Hypothetically, the ADC response after RE could be delayed and of a different character than the ADC response after HAE.

Also, ultrasonographic elastography (ARFI) for evaluation of inflammatory response after treatments have been performed, and these data need to be analysed. The observed increase of ALP in RE patients could be linked to radiation related damages on the vascular endothelium also seen in RILD, but to a lesser extent. A platelet activation and aggregation leading to accumulation of fibrine and fibroblast proliferation can possibly then be visualized in the ARFI investigations (179, 180).

Finally, quality-of-life questionnaires have been collected and will be analysed for differences before and after treatment and between HAE and RE.

TACK!

In so many ways have so many people contributed to this thesis. I want to express my warm and sincere gratitude to all of you! Some of you I would like to thank with more words:

Viktor Johanson, my main supervisor and colleague, for your contagious curiosity of how things work and for your support, always. You have an impressive sense of details in both our research and surgery in the clinic. I have learnt so much from you and because of you. I am so grateful for having spent this journey with you!

Co-supervisor **Bo Wängberg** for your calm and positive attitude. For sharing your great knowledge in so many fields and for firm belief in me during tough times.

Co-supervisor **Peter Bernhardt** for always so interesting discussions, that in some way made me understand a glimpse of radiophysics. I am so happy to be on your team and hopefully we will share more exciting projects in the future!

Erik Elias, for adding new energy and creative thoughts to our research group. For always giving me inspiration to continue when doubts come, and suggesting new directions when needed.

Mats Andersson for quick and excellent hard work with our paper, for sharing your great knowledge and answering all my questions.

Oscar Jalnefjord for adding an extra-ordinary sharp mind and for making extremely complicated physical stuff a little less diffuse.

Ida Marin for always making time for me and for helpful discussions.

Johanna Svensson and **Rauni Rossi Norrlund** for enthusiasm, encouragement and fun and interesting discussions. I hope many joint projects lie ahead of us.

Olof Henriksson and **Maria Ljungberg** for support and professional work.

Maria Nilsson and **Kajsa Holgersson,** for always positive and friendly help!

Anders Bergström for hard work even in a stressful situation, and for letting me use your beautiful photos! **Ola Nilsson** for adding your vast knowledge in pathology and sharp sense of how to complete a paper.

Yvonne Arvidsson, Tobias Hofving, Gülay Altiparmak and **Linda Inge** at the Sahlgrenska Cancer Center for creating an inspiring environment at the Lab.

All friends and hard-working colleagues at the Department of Surgery at Sahlgrenska University Hospital for cheerful support, sympathy when needed and for making our department a nice place to be. Special thoughts to the whole Endocrine Surgery Unit for being a great team, which I am proud to be a member of.

Peter Naredi, Professor of Surgery and head of the Institution of Clinical Sciences, for time to fulfil this project.

Mom and Dad for love and support, teaching me the importance of knowledge and for making me the one I am. Love to my brothers **Mats** and **Tomas**.

Klara and Amanda for being there. You fill me with joy and inspiration!

Saga, Sixten and Valdemar for always bringing sunshine on a rainy day and for overwhelming hugs. For patience, understanding and everlasting support during this project, that was so important to me. Thank you, Saga - you turned the cover into a piece of art!

Last but most important: **Lars**, for endless pep talks, technical expertise, warm hugs and keeping it all together during tough times. I love you!

The work presented in this thesis was supported by Sahlgrenska Academy (ALF agreement), Biocare Grants, the Assar Gabrielsson Research Foundation, Wilhelm and Martina Lundgren Foundation, Knut and Alice Wallenberg Foundation and the Swedish Cancer Society.

REFERENCES

1. Tischler AS. The dispersed neuroendocrine cells: the structure, function, regulation and effects of xenobiotics on this system. Toxicologic pathology. 1989;17(2):307-16.
2. Modlin IM, Oberg K, Chung DC, Jensen RT, de Herder WW, Thakker RV, et al. Gastroenteropancreatic neuroendocrine tumours. The Lancet Oncology. 2008;9(1):61-72.
3. Ito T, Igarashi H, Nakamura K, Sasano H, Okusaka T, Takano K, et al. Epidemiological trends of pancreatic and gastrointestinal neuroendocrine tumors in Japan: a nationwide survey analysis. Journal of gastroenterology. 2015;50(1):58-64.
4. Lepage C, Bouvier AM, Faivre J. Endocrine tumours: epidemiology of malignant digestive neuroendocrine tumours. European journal of endocrinology. 2013;168(4):R77-83.
5. Berge T, Linell F. Carcinoid tumours. Frequency in a defined population during a 12-year period. Acta pathologica et microbiologica Scandinavica Section A, Pathology. 1976;84(4):322-30.
6. Yao JC, Hassan M, Phan A, Dagohoy C, Leary C, Mares JE, et al. One hundred years after "carcinoid": epidemiology of and prognostic factors for neuroendocrine tumors in 35,825 cases in the United States. Journal of clinical oncology : official journal of the American Society of Clinical Oncology. 2008;26(18):3063-72.
7. Laskaratos FM, Rombouts K, Caplin M, Toumpanakis C, Thirlwell C, Mandair D. Neuroendocrine tumors and fibrosis: An unsolved mystery? Cancer. 2017;123(24):4770-90.
8. Modlin IM, Bodei L, Kidd M. Neuroendocrine tumor biomarkers: From monoanalytes to transcripts and algorithms. Best practice & research Clinical endocrinology & metabolism. 2016;30(1):59-77.
9. Modlin IM, Kidd M, Latich I, Zikusoka MN, Shapiro MD. Current status of gastrointestinal carcinoids. Gastroenterology. 2005;128(6):1717-51.
10. Hedenstrom P, Marschall HU, Nilsson B, Demir A, Lindkvist B, Nilsson O, et al. High clinical impact and diagnostic accuracy of EUS-guided biopsy sampling of subepithelial lesions: a prospective, comparative study. Surgical endoscopy. 2018;32(3):1304-13.
11. Tang LH, Gonen M, Hedvat C, Modlin IM, Klimstra DS. Objective quantification of the Ki67 proliferative index in neuroendocrine tumors of the gastroenteropancreatic system: a comparison of digital image analysis with manual methods. The American journal of surgical pathology. 2012;36(12):1761-70.
12. Pape UF, Jann H, Muller-Nordhorn J, Bockelbrink A, Berndt U, Willich SN, et al. Prognostic relevance of a novel TNM classification system for upper gastroenteropancreatic neuroendocrine tumors. Cancer. 2008;113(2):256-65.
13. Strosberg J, Nasir A, Coppola D, Wick M, Kvols L. Correlation between grade and prognosis in metastatic gastroenteropancreatic neuroendocrine tumors. Human pathology. 2009;40(9):1262-8.

14. Kloppel G, Couvelard A, Perren A, Komminoth P, McNicol AM, Nilsson O, et al. ENETS Consensus Guidelines for the Standards of Care in Neuroendocrine Tumors: towards a standardized approach to the diagnosis of gastroenteropancreatic neuroendocrine tumors and their prognostic stratification. Neuroendocrinology. 2009;90(2):162-6.
15. Perren A, Couvelard A, Scoazec JY, Costa F, Borbath I, Delle Fave G, et al. ENETS Consensus Guidelines for the Standards of Care in Neuroendocrine Tumors: Pathology: Diagnosis and Prognostic Stratification. Neuroendocrinology. 2017;105(3):196-200.
16. Riihimaki M, Hemminki A, Sundquist K, Sundquist J, Hemminki K. The epidemiology of metastases in neuroendocrine tumors. International journal of cancer. 2016;139(12):2679-86.
17. Jann H, Roll S, Couvelard A, Hentic O, Pavel M, Muller-Nordhorn J, et al. Neuroendocrine tumors of midgut and hindgut origin: tumor-node-metastasis classification determines clinical outcome. Cancer. 2011;117(15):3332-41.
18. Niederle B, Pape UF, Costa F, Gross D, Kelestimur F, Knigge U, et al. ENETS Consensus Guidelines Update for Neuroendocrine Neoplasms of the Jejunum and Ileum. Neuroendocrinology. 2016;103(2):125-38.
19. Hellman P, Lundstrom T, Ohrvall U, Eriksson B, Skogseid B, Oberg K, et al. Effect of surgery on the outcome of midgut carcinoid disease with lymph node and liver metastases. World journal of surgery. 2002;26(8):991-7.
20. Daskalakis K, Karakatsanis A, Hessman O, Stuart HC, Welin S, Tiensuu Janson E, et al. Association of a Prophylactic Surgical Approach to Stage IV Small Intestinal Neuroendocrine Tumors With Survival. JAMA oncology. 2018;4(2):183-9.
21. Bettini R, Partelli S, Boninsegna L, Capelli P, Crippa S, Pederzoli P, et al. Tumor size correlates with malignancy in nonfunctioning pancreatic endocrine tumor. Surgery. 2011;150(1):75-82.
22. Lee LC, Grant CS, Salomao DR, Fletcher JG, Takahashi N, Fidler JL, et al. Small, nonfunctioning, asymptomatic pancreatic neuroendocrine tumors (PNETs): role for nonoperative management. Surgery. 2012;152(6):965-74.
23. Falconi M, Plockinger U, Kwekkeboom DJ, Manfredi R, Korner M, Kvols L, et al. Well-differentiated pancreatic nonfunctioning tumors/carcinoma. Neuroendocrinology. 2006;84(3):196-211.
24. Zerbi A, Falconi M, Rindi G, Delle Fave G, Tomassetti P, Pasquali C, et al. Clinicopathological features of pancreatic endocrine tumors: a prospective multicenter study in Italy of 297 sporadic cases. The American journal of gastroenterology. 2010;105(6):1421-9.
25. Falconi M, Eriksson B, Kaltsas G, Bartsch DK, Capdevila J, Caplin M, et al. ENETS Consensus Guidelines Update for the Management of Patients with Functional Pancreatic Neuroendocrine Tumors and Non-Functional Pancreatic Neuroendocrine Tumors. Neuroendocrinology. 2016;103(2):153-71.
26. Garcia-Carbonero R, Rinke A, Valle JW, Fazio N, Caplin M, Gorbounova V, et al. ENETS Consensus Guidelines for the Standards of Care in

Neuroendocrine Neoplasms. Systemic Therapy 2: Chemotherapy. Neuroendocrinology. 2017;105(3):281-94.
27. Yao JC, Fazio N, Singh S, Buzzoni R, Carnaghi C, Wolin E, et al. Everolimus for the treatment of advanced, non-functional neuroendocrine tumours of the lung or gastrointestinal tract (RADIANT-4): a randomised, placebo-controlled, phase 3 study. Lancet (London, England). 2016;387(10022):968-77.
28. Raymond E, Dahan L, Raoul JL, Bang YJ, Borbath I, Lombard-Bohas C, et al. Sunitinib malate for the treatment of pancreatic neuroendocrine tumors. The New England journal of medicine. 2011;364(6):501-13.
29. Pavel M, Baudin E, Couvelard A, Krenning E, Oberg K, Steinmuller T, et al. ENETS Consensus Guidelines for the management of patients with liver and other distant metastases from neuroendocrine neoplasms of foregut, midgut, hindgut, and unknown primary. Neuroendocrinology. 2012;95(2):157-76.
30. Tamburrino D, Spoletini G, Partelli S, Muffatti F, Adamenko O, Crippa S, et al. Surgical management of neuroendocrine tumors. Best practice & research Clinical endocrinology & metabolism. 2016;30(1):93-102.
31. Frilling A, Modlin IM, Kidd M, Russell C, Breitenstein S, Salem R, et al. Recommendations for management of patients with neuroendocrine liver metastases. The Lancet Oncology. 2014;15(1):e8-21.
32. Mayo SC, de Jong MC, Pulitano C, Clary BM, Reddy SK, Gamblin TC, et al. Surgical management of hepatic neuroendocrine tumor metastasis: results from an international multi-institutional analysis. Annals of surgical oncology. 2010;17(12):3129-36.
33. Touzios JG, Kiely JM, Pitt SC, Rilling WS, Quebbeman EJ, Wilson SD, et al. Neuroendocrine hepatic metastases: does aggressive management improve survival? Annals of surgery. 2005;241(5):776-83; discussion 83-5.
34. Olausson M, Friman S, Herlenius G, Cahlin C, Nilsson O, Jansson S, et al. Orthotopic liver or multivisceral transplantation as treatment of metastatic neuroendocrine tumors. Liver transplantation : official publication of the American Association for the Study of Liver Diseases and the International Liver Transplantation Society. 2007;13(3):327-33.
35. Fan ST, Le Treut YP, Mazzaferro V, Burroughs AK, Olausson M, Breitenstein S, et al. Liver transplantation for neuroendocrine tumour liver metastases. HPB : the official journal of the International Hepato Pancreato Biliary Association. 2015;17(1):23-8.
36. Kennedy A, Bester L, Salem R, Sharma RA, Parks RW, Ruszniewski P. Role of hepatic intra-arterial therapies in metastatic neuroendocrine tumours (NET): guidelines from the NET-Liver-Metastases Consensus Conference. HPB : the official journal of the International Hepato Pancreato Biliary Association. 2015;17(1):29-37.
37. Vogl TJ, Naguib NN, Zangos S, Eichler K, Hedayati A, Nour-Eldin NE. Liver metastases of neuroendocrine carcinomas: interventional treatment via transarterial embolization, chemoembolization and thermal ablation. European journal of radiology. 2009;72(3):517-28.

38. Mohan H, Nicholson P, Winter DC, O'Shea D, O'Toole D, Geoghegan J, et al. Radiofrequency ablation for neuroendocrine liver metastases: a systematic review. Journal of vascular and interventional radiology : JVIR. 2015;26(7):935-42.e1.
39. Eriksson J, Stalberg P, Nilsson A, Krause J, Lundberg C, Skogseid B, et al. Surgery and radiofrequency ablation for treatment of liver metastases from midgut and foregut carcinoids and endocrine pancreatic tumors. World journal of surgery. 2008;32(5):930-8.
40. Norlen O, Stalberg P, Zedenius J, Hellman P. Outcome after resection and radiofrequency ablation of liver metastases from small intestinal neuroendocrine tumours. The British journal of surgery. 2013;100(11):1505-14.
41. Chuang VP, Wallace S. Hepatic artery embolization in the treatment of hepatic neoplasms. Radiology. 1981;140(1):51-8.
42. Del Prete M, Fiore F, Modica R, Marotta V, Marciello F, Ramundo V, et al. Hepatic arterial embolization in patients with neuroendocrine tumors. Journal of experimental & clinical cancer research : CR. 2014;33:43.
43. Lewis MA, Jaramillo S, Roberts L, Fleming CJ, Rubin J, Grothey A. Hepatic artery embolization for neuroendocrine tumors: postprocedural management and complications. The oncologist. 2012;17(5):725-31.
44. Proye C. Natural history of liver metastasis of gastroenteropancreatic neuroendocrine tumors: place for chemoembolization. World journal of surgery. 2001;25(6):685-8.
45. King J, Quinn R, Glenn DM, Janssen J, Tong D, Liaw W, et al. Radioembolization with selective internal radiation microspheres for neuroendocrine liver metastases. Cancer. 2008;113(5):921-9.
46. Rhee TK, Lewandowski RJ, Liu DM, Mulcahy MF, Takahashi G, Hansen PD, et al. 90Y Radioembolization for metastatic neuroendocrine liver tumors: preliminary results from a multi-institutional experience. Annals of surgery. 2008;247(6):1029-35.
47. Zappa M, Abdel-Rehim M, Hentic O, Vullierme MP, Ruszniewski P, Vilgrain V. Liver-directed therapies in liver metastases from neuroendocrine tumors of the gastrointestinal tract. Targeted oncology. 2012;7(2):107-16.
48. Lewis MA, Hobday TJ. Treatment of neuroendocrine tumor liver metastases. International journal of hepatology. 2012;2012:973946.
49. Sward C, Johanson V, Nieveen van Dijkum E, Jansson S, Nilsson O, Wangberg B, et al. Prolonged survival after hepatic artery embolization in patients with midgut carcinoid syndrome. The British journal of surgery. 2009;96(5):517-21.
50. Kennedy A, Coldwell D, Sangro B, Wasan H, Salem R. Integrating radioembolization into the treatment paradigm for metastatic neuroendocrine tumors in the liver. American journal of clinical oncology. 2012;35(4):393-8.
51. Gupta S, Johnson MM, Murthy R, Ahrar K, Wallace MJ, Madoff DC, et al. Hepatic arterial embolization and chemoembolization for the treatment of patients with metastatic neuroendocrine tumors: variables affecting response rates and survival. Cancer. 2005;104(8):1590-602.
52. Fiore F, Del Prete M, Franco R, Marotta V, Ramundo V, Marciello F, et al. Transarterial embolization (TAE) is equally effective and slightly safer than

transarterial chemoembolization (TACE) to manage liver metastases in neuroendocrine tumors. Endocrine. 2014;47(1):177-82.
53. Engelman ES, Leon-Ferre R, Naraev BG, Sharma N, Sun S, O'Dorisio TM, et al. Comparison of transarterial liver-directed therapies for low-grade metastatic neuroendocrine tumors in a single institution. Pancreas. 2014;43(2):219-25.
54. Reubi JC, Waser B. Concomitant expression of several peptide receptors in neuroendocrine tumours: molecular basis for in vivo multireceptor tumour targeting. European journal of nuclear medicine and molecular imaging. 2003;30(5):781-93.
55. Krenning EP, Kwekkeboom DJ, Bakker WH, Breeman WA, Kooij PP, Oei HY, et al. Somatostatin receptor scintigraphy with [111In-DTPA-D-Phe1]- and [123I-Tyr3]-octreotide: the Rotterdam experience with more than 1000 patients. European journal of nuclear medicine. 1993;20(8):716-31.
56. Patel YC. Somatostatin and its receptor family. Frontiers in neuroendocrinology. 1999;20(3):157-98.
57. Bauer W, Briner U, Doepfner W, Haller R, Huguenin R, Marbach P, et al. SMS 201-995: a very potent and selective octapeptide analogue of somatostatin with prolonged action. Life sciences. 1982;31(11):1133-40.
58. Wolin EM. The expanding role of somatostatin analogs in the management of neuroendocrine tumors. Gastrointestinal cancer research : GCR. 2012;5(5):161-8.
59. Schmid HA. Pasireotide (SOM230): development, mechanism of action and potential applications. Molecular and cellular endocrinology. 2008;286(1-2):69-74.
60. de Herder WW, van der Lely AJ, Lamberts SW. Somatostatin analogue treatment of neuroendocrine tumours. Postgraduate medical journal. 1996;72(849):403-8.
61. Rinke A, Muller HH, Schade-Brittinger C, Klose KJ, Barth P, Wied M, et al. Placebo-controlled, double-blind, prospective, randomized study on the effect of octreotide LAR in the control of tumor growth in patients with metastatic neuroendocrine midgut tumors: a report from the PROMID Study Group. Journal of clinical oncology : official journal of the American Society of Clinical Oncology. 2009;27(28):4656-63.
62. Caplin ME, Pavel M, Cwikla JB, Phan AT, Raderer M, Sedlackova E, et al. Lanreotide in metastatic enteropancreatic neuroendocrine tumors. The New England journal of medicine. 2014;371(3):224-33.
63. Lamberts SW, Chayvialle JA, Krenning EP. The visualization of gastroenteropancreatic endocrine tumors. Metabolism: clinical and experimental. 1992;41(9 Suppl 2):111-5.
64. Buchmann I, Henze M, Engelbrecht S, Eisenhut M, Runz A, Schafer M, et al. Comparison of 68Ga-DOTATOC PET and 111In-DTPAOC (Octreoscan) SPECT in patients with neuroendocrine tumours. European journal of nuclear medicine and molecular imaging. 2007;34(10):1617-26.
65. Van Binnebeek S, Vanbilloen B, Baete K, Terwinghe C, Koole M, Mottaghy FM, et al. Comparison of diagnostic accuracy of (111)In-pentetreotide

SPECT and (68)Ga-DOTATOC PET/CT: A lesion-by-lesion analysis in patients with metastatic neuroendocrine tumours. European radiology. 2016;26(3):900-9.
66. Krenning EP, Kooij PP, Pauwels S, Breeman WA, Postema PT, De Herder WW, et al. Somatostatin receptor: scintigraphy and radionuclide therapy. Digestion. 1996;57 Suppl 1:57-61.
67. Fjalling M, Andersson P, Forssell-Aronsson E, Gretarsdottir J, Johansson V, Tisell LE, et al. Systemic radionuclide therapy using indium-111-DTPA-D-Phe1-octreotide in midgut carcinoid syndrome. Journal of nuclear medicine : official publication, Society of Nuclear Medicine. 1996;37(9):1519-21.
68. Uusijarvi H, Bernhardt P, Ericsson T, Forssell-Aronsson E. Dosimetric characterization of radionuclides for systemic tumor therapy: influence of particle range, photon emission, and subcellular distribution. Medical physics. 2006;33(9):3260-9.
69. O'Donoghue JA, Bardies M, Wheldon TE. Relationships between tumor size and curability for uniformly targeted therapy with beta-emitting radionuclides. Journal of nuclear medicine : official publication, Society of Nuclear Medicine. 1995;36(10):1902-9.
70. Bernhardt P, Ahlman H, Forssell-Aronsson E. Model of metastatic growth valuable for radionuclide therapy. Medical physics. 2003;30(12):3227-32.
71. Bodei L, Cremonesi M, Ferrari M, Pacifici M, Grana CM, Bartolomei M, et al. Long-term evaluation of renal toxicity after peptide receptor radionuclide therapy with 90Y-DOTATOC and 177Lu-DOTATATE: the role of associated risk factors. European journal of nuclear medicine and molecular imaging. 2008;35(10):1847-56.
72. Valkema R, Pauwels SA, Kvols LK, Kwekkeboom DJ, Jamar F, de Jong M, et al. Long-term follow-up of renal function after peptide receptor radiation therapy with (90)Y-DOTA(0),Tyr(3)-octreotide and (177)Lu-DOTA(0), Tyr(3)-octreotate. Journal of nuclear medicine : official publication, Society of Nuclear Medicine. 2005;46 Suppl 1:83s-91s.
73. Kwekkeboom DJ, Kooij PP, Bakker WH, Macke HR, Krenning EP. Comparison of 111In-DOTA-Tyr3-octreotide and 111In-DTPA-octreotide in the same patients: biodistribution, kinetics, organ and tumor uptake. Journal of nuclear medicine : official publication, Society of Nuclear Medicine. 1999;40(5):762-7.
74. Reubi JC, Schar JC, Waser B, Wenger S, Heppeler A, Schmitt JS, et al. Affinity profiles for human somatostatin receptor subtypes SST1-SST5 of somatostatin radiotracers selected for scintigraphic and radiotherapeutic use. European journal of nuclear medicine. 2000;27(3):273-82.
75. Sward C, Bernhardt P, Johanson V, Schmitt A, Ahlman H, Stridsberg M, et al. Comparison of [177Lu-DOTA0,Tyr3]-octreotate and [177Lu-DOTA0,Tyr3]-octreotide for receptor-mediated radiation therapy of the xenografted human midgut carcinoid tumor GOT1. Cancer biotherapy & radiopharmaceuticals. 2008;23(1):114-20.
76. Kwekkeboom DJ, de Herder WW, Kam BL, van Eijck CH, van Essen M, Kooij PP, et al. Treatment with the radiolabeled somatostatin analog [177 Lu-

DOTA 0,Tyr3]octreotate: toxicity, efficacy, and survival. Journal of clinical oncology : official journal of the American Society of Clinical Oncology. 2008;26(13):2124-30.
77. Bodei L, Kidd M, Paganelli G, Grana CM, Drozdov I, Cremonesi M, et al. Long-term tolerability of PRRT in 807 patients with neuroendocrine tumours: the value and limitations of clinical factors. European journal of nuclear medicine and molecular imaging. 2015;42(1):5-19.
78. Sabet A, Ezziddin K, Pape UF, Ahmadzadehfar H, Mayer K, Poppel T, et al. Long-term hematotoxicity after peptide receptor radionuclide therapy with 177Lu-octreotate. Journal of nuclear medicine : official publication, Society of Nuclear Medicine. 2013;54(11):1857-61.
79. Sandstrom M, Garske-Roman U, Granberg D, Johansson S, Widstrom C, Eriksson B, et al. Individualized dosimetry of kidney and bone marrow in patients undergoing 177Lu-DOTA-octreotate treatment. Journal of nuclear medicine : official publication, Society of Nuclear Medicine. 2013;54(1):33-41.
80. Svensson J, Berg G, Wangberg B, Larsson M, Forssell-Aronsson E, Bernhardt P. Renal function affects absorbed dose to the kidneys and haematological toxicity during (1)(7)(7)Lu-DOTATATE treatment. European journal of nuclear medicine and molecular imaging. 2015;42(6):947-55.
81. Rolleman EJ, Melis M, Valkema R, Boerman OC, Krenning EP, de Jong M. Kidney protection during peptide receptor radionuclide therapy with somatostatin analogues. European journal of nuclear medicine and molecular imaging. 2010;37(5):1018-31.
82. Kwekkeboom DJ, Teunissen JJ, Bakker WH, Kooij PP, de Herder WW, Feelders RA, et al. Radiolabeled somatostatin analog [177Lu-DOTA0,Tyr3]octreotate in patients with endocrine gastroenteropancreatic tumors. Journal of clinical oncology : official journal of the American Society of Clinical Oncology. 2005;23(12):2754-62.
83. Ezziddin S, Attassi M, Yong-Hing CJ, Ahmadzadehfar H, Willinek W, Grunwald F, et al. Predictors of long-term outcome in patients with well-differentiated gastroenteropancreatic neuroendocrine tumors after peptide receptor radionuclide therapy with 177Lu-octreotate. Journal of nuclear medicine : official publication, Society of Nuclear Medicine. 2014;55(2):183-90.
84. Bodei L, Cremonesi M, Grana CM, Fazio N, Iodice S, Baio SM, et al. Peptide receptor radionuclide therapy with (1)(7)(7)Lu-DOTATATE: the IEO phase I-II study. European journal of nuclear medicine and molecular imaging. 2011;38(12):2125-35.
85. Garske-Roman U, Sandstrom M, Fross Baron K, Lundin L, Hellman P, Welin S, et al. Prospective observational study of (177)Lu-DOTA-octreotate therapy in 200 patients with advanced metastasized neuroendocrine tumours (NETs): feasibility and impact of a dosimetry-guided study protocol on outcome and toxicity. European journal of nuclear medicine and molecular imaging. 2018;45(6):970-88.
86. Teunissen JJ, Kwekkeboom DJ, Krenning EP. Quality of life in patients with gastroenteropancreatic tumors treated with [177Lu-DOTA0,Tyr3]octreotate. Journal of clinical oncology : official journal of the American Society of Clinical Oncology. 2004;22(13):2724-9.

87. Kolby L, Bernhardt P, Johanson V, Schmitt A, Ahlman H, Forssell-Aronsson E, et al. Successful receptor-mediated radiation therapy of xenografted human midgut carcinoid tumour. British journal of cancer. 2005;93(10):1144-51.
88. Strosberg J, El-Haddad G, Wolin E, Hendifar A, Yao J, Chasen B, et al. Phase 3 Trial of (177)Lu-Dotatate for Midgut Neuroendocrine Tumors. The New England journal of medicine. 2017;376(2):125-35.
89. Otte A, Herrmann R, Heppeler A, Behe M, Jermann E, Powell P, et al. Yttrium-90 DOTATOC: first clinical results. European journal of nuclear medicine. 1999;26(11):1439-47.
90. Emami B, Lyman J, Brown A, Coia L, Goitein M, Munzenrider JE, et al. Tolerance of normal tissue to therapeutic irradiation. International journal of radiation oncology, biology, physics. 1991;21(1):109-22.
91. Bergsma H, Konijnenberg MW, Kam BL, Teunissen JJ, Kooij PP, de Herder WW, et al. Subacute haematotoxicity after PRRT with (177)Lu-DOTA-octreotate: prognostic factors, incidence and course. European journal of nuclear medicine and molecular imaging. 2016;43(3):453-63.
92. Shahidi M, Mozdarani H, Bryant PE. Radiation sensitivity of leukocytes from healthy individuals and breast cancer patients as measured by the alkaline and neutral comet assay. Cancer letters. 2007;257(2):263-73.
93. Shahidi M, Mozdarani H, Mueller WU. Radiosensitivity and repair kinetics of gamma-irradiated leukocytes from sporadic prostate cancer patients and healthy individuals assessed by alkaline comet assay. Iranian biomedical journal. 2010;14(3):67-75.
94. Jonathan EC, Bernhard EJ, McKenna WG. How does radiation kill cells? Current opinion in chemical biology. 1999;3(1):77-83.
95. Connell PP, Hellman S. Advances in radiotherapy and implications for the next century: a historical perspective. Cancer research. 2009;69(2):383-92.
96. Chiarugi A, Dolle C, Felici R, Ziegler M. The NAD metabolome--a key determinant of cancer cell biology. Nature reviews Cancer. 2012;12(11):741-52.
97. Schreiber V, Dantzer F, Ame JC, de Murcia G. Poly(ADP-ribose): novel functions for an old molecule. Nature reviews Molecular cell biology. 2006;7(7):517-28.
98. Watson M, Roulston A, Belec L, Billot X, Marcellus R, Bedard D, et al. The small molecule GMX1778 is a potent inhibitor of NAD+ biosynthesis: strategy for enhanced therapy in nicotinic acid phosphoribosyltransferase 1-deficient tumors. Molecular and cellular biology. 2009;29(21):5872-88.
99. Johanson V, Arvidsson Y, Kolby L, Bernhardt P, Sward C, Nilsson O, et al. Antitumoural effects of the pyridyl cyanoguanidine CHS 828 on three different types of neuroendocrine tumours xenografted to nude mice. Neuroendocrinology. 2005;82(3-4):171-6.
100. Kato H, Ito E, Shi W, Alajez NM, Yue S, Lee C, et al. Efficacy of combining GMX1777 with radiation therapy for human head and neck carcinoma. Clinical cancer research : an official journal of the American Association for Cancer Research. 2010;16(3):898-911.

101. Kong G, Johnston V, Ramdave S, Lau E, Rischin D, Hicks RJ. High-administered activity In-111 octreotide therapy with concomitant radiosensitizing 5FU chemotherapy for treatment of neuroendocrine tumors: preliminary experience. Cancer biotherapy & radiopharmaceuticals. 2009;24(5):527-33.
102. Kashyap R, Hofman MS, Michael M, Kong G, Akhurst T, Eu P, et al. Favourable outcomes of (177)Lu-octreotate peptide receptor chemoradionuclide therapy in patients with FDG-avid neuroendocrine tumours. European journal of nuclear medicine and molecular imaging. 2015;42(2):176-85.
103. van Essen M, Krenning EP, Kam BL, de Herder WW, van Aken MO, Kwekkeboom DJ. Report on short-term side effects of treatments with 177Lu-octreotate in combination with capecitabine in seven patients with gastroenteropancreatic neuroendocrine tumours. European journal of nuclear medicine and molecular imaging. 2008;35(4):743-8.
104. Claringbold PG, Price RA, Turner JH. Phase I-II study of radiopeptide 177Lu-octreotate in combination with capecitabine and temozolomide in advanced low-grade neuroendocrine tumors. Cancer biotherapy & radiopharmaceuticals. 2012;27(9):561-9.
105. Kolby L, Bernhardt P, Sward C, Johanson V, Ahlman H, Forssell-Aronsson E, et al. Chromogranin A as a determinant of midgut carcinoid tumour volume. Regulatory peptides. 2004;120(1-3):269-73.
106. Yao JC, Pavel M, Phan AT, Kulke MH, Hoosen S, St Peter J, et al. Chromogranin A and neuron-specific enolase as prognostic markers in patients with advanced pNET treated with everolimus. The Journal of clinical endocrinology and metabolism. 2011;96(12):3741-9.
107. Bodei L, Kidd M, Modlin IM, Severi S, Drozdov I, Nicolini S, et al. Measurement of circulating transcripts and gene cluster analysis predicts and defines therapeutic efficacy of peptide receptor radionuclide therapy (PRRT) in neuroendocrine tumors. European journal of nuclear medicine and molecular imaging. 2016;43(5):839-51.
108. Marotta V, Zatelli MC, Sciammarella C, Ambrosio MR, Bondanelli M, Colao A, et al. Chromogranin A as circulating marker for diagnosis and management of neuroendocrine neoplasms: more flaws than fame. Endocrine-related cancer. 2018;25(1):R11-r29.
109. Oberg K, Krenning E, Sundin A, Bodei L, Kidd M, Tesselaar M, et al. A Delphic consensus assessment: imaging and biomarkers in gastroenteropancreatic neuroendocrine tumor disease management. Endocrine connections. 2016;5(5):174-87.
110. Eisenhauer EA, Therasse P, Bogaerts J, Schwartz LH, Sargent D, Ford R, et al. New response evaluation criteria in solid tumours: revised RECIST guideline (version 1.1). European journal of cancer (Oxford, England : 1990). 2009;45(2):228-47.
111. de Mestier L, Dromain C, d'Assignies G, Scoazec JY, Lassau N, Lebtahi R, et al. Evaluating digestive neuroendocrine tumor progression and therapeutic responses in the era of targeted therapies: state of the art. Endocrine-related cancer. 2014;21(3):R105-20.

112. Luo Y, Chen J, Huang K, Lin Y, Chen M, Xu L, et al. Early evaluation of sunitinib for the treatment of advanced gastroenteropancreatic neuroendocrine neoplasms via CT imaging: RECIST 1.1 or Choi Criteria? BMC cancer. 2017;17(1):154.
113. Taouli B, Koh DM. Diffusion-weighted MR imaging of the liver. Radiology. 2010;254(1):47-66.
114. Dudeck O, Zeile M, Wybranski C, Schulmeister A, Fischbach F, Pech M, et al. Early prediction of anticancer effects with diffusion-weighted MR imaging in patients with colorectal liver metastases following selective internal radiotherapy. European radiology. 2010;20(11):2699-706.
115. Sundin A, Rockall A. Therapeutic monitoring of gastroenteropancreatic neuroendocrine tumors: the challenges ahead. Neuroendocrinology. 2012;96(4):261-71.
116. Kukuk GM, Murtz P, Traber F, Meyer C, Ullrich J, Gieseke J, et al. Diffusion-weighted imaging with acquisition of three b-values for response evaluation of neuroendocrine liver metastases undergoing selective internal radiotherapy. European radiology. 2014;24(2):267-76.
117. Gowdra Halappa V, Corona-Villalobos CP, Bonekamp S, Li Z, Reyes D, Cosgrove D, et al. Neuroendocrine liver metastasis treated by using intraarterial therapy: volumetric functional imaging biomarkers of early tumor response and survival. Radiology. 2013;266(2):502-13.
118. Kartalis N, Mucelli RM, Sundin A. Recent developments in imaging of pancreatic neuroendocrine tumors. Annals of gastroenterology. 2015;28(2):193-202.
119. Guo Y, Yaghmai V, Salem R, Lewandowski RJ, Nikolaidis P, Larson AC, et al. Imaging tumor response following liver-directed intra-arterial therapy. Abdominal imaging. 2013;38(6):1286-99.
120. Gonzalez-Guindalini FD, Botelho MP, Harmath CB, Sandrasegaran K, Miller FH, Salem R, et al. Assessment of liver tumor response to therapy: role of quantitative imaging. Radiographics : a review publication of the Radiological Society of North America, Inc. 2013;33(6):1781-800.
121. Sgouros G. Dosimetry of internal emitters. Journal of nuclear medicine : official publication, Society of Nuclear Medicine. 2005;46 Suppl 1:18s-27s.
122. Larsson M, Bernhardt P, Svensson JB, Wangberg B, Ahlman H, Forssell-Aronsson E. Estimation of absorbed dose to the kidneys in patients after treatment with 177Lu-octreotate: comparison between methods based on planar scintigraphy. EJNMMI research. 2012;2(1):49.
123. Norrgren K, Svegborn SL, Areberg J, Mattsson S. Accuracy of the quantification of organ activity from planar gamma camera images. Cancer biotherapy & radiopharmaceuticals. 2003;18(1):125-31.
124. Magnander T, Svensson J, Bath M, Gjertsson P, Bernhardt P. IMPROVED PLANAR KIDNEY ACTIVITY CONCENTRATION ESTIMATE BY THE POSTERIOR VIEW METHOD IN 177LU-DOTATATE TREATMENTS. Radiation protection dosimetry. 2016;169(1-4):259-66.

125. Eckerman K, Endo A. ICRP Publication 107. Nuclear decay data for dosimetric calculations. Annals of the ICRP. 2008;38(3):7-96.
126. Garkavij M, Nickel M, Sjogreen-Gleisner K, Ljungberg M, Ohlsson T, Wingardh K, et al. 177Lu-[DOTA0,Tyr3] octreotate therapy in patients with disseminated neuroendocrine tumors: Analysis of dosimetry with impact on future therapeutic strategy. Cancer. 2010;116(4 Suppl):1084-92.
127. Ilan E, Sandstrom M, Wassberg C, Sundin A, Garske-Roman U, Eriksson B, et al. Dose response of pancreatic neuroendocrine tumors treated with peptide receptor radionuclide therapy using 177Lu-DOTATATE. Journal of nuclear medicine : official publication, Society of Nuclear Medicine. 2015;56(2):177-82.
128. Cremonesi M, Chiesa C, Strigari L, Ferrari M, Botta F, Guerriero F, et al. Radioembolization of hepatic lesions from a radiobiology and dosimetric perspective. Frontiers in oncology. 2014;4:210.
129. Bernardini M, Smadja C, Faraggi M, Orio S, Petitguillaume A, Desbree A, et al. Liver Selective Internal Radiation Therapy with (90)Y resin microspheres: comparison between pre-treatment activity calculation methods. Physica medica : PM : an international journal devoted to the applications of physics to medicine and biology : official journal of the Italian Association of Biomedical Physics (AIFB). 2014;30(7):752-64.
130. Ahmadzadehfar H, Muckle M, Sabet A, Wilhelm K, Kuhl C, Biermann K, et al. The significance of bremsstrahlung SPECT/CT after yttrium-90 radioembolization treatment in the prediction of extrahepatic side effects. European journal of nuclear medicine and molecular imaging. 2012;39(2):309-15.
131. Lhommel R, van Elmbt L, Goffette P, Van den Eynde M, Jamar F, Pauwels S, et al. Feasibility of 90Y TOF PET-based dosimetry in liver metastasis therapy using SIR-Spheres. European journal of nuclear medicine and molecular imaging. 2010;37(9):1654-62.
132. Ryden T, Heydorn Lagerlof J, Hemmingsson J, Marin I, Svensson J, Bath M, et al. Fast GPU-based Monte Carlo code for SPECT/CT reconstructions generates improved (177)Lu images. EJNMMI physics. 2018;5(1):1.
133. Arvidsson Y, Rehammar A, Bergstrom A, Andersson E, Altiparmak G, Sward C, et al. miRNA profiling of small intestinal neuroendocrine tumors defines novel molecular subtypes and identifies miR-375 as a biomarker of patient survival. Modern pathology : an official journal of the United States and Canadian Academy of Pathology, Inc. 2018.
134. Specht E, Kaemmerer D, Sanger J, Wirtz RM, Schulz S, Lupp A. Comparison of immunoreactive score, HER2/neu score and H score for the immunohistochemical evaluation of somatostatin receptors in bronchopulmonary neuroendocrine neoplasms. Histopathology. 2015;67(3):368-77.
135. Kolby L, Bernhardt P, Ahlman H, Wangberg B, Johanson V, Wigander A, et al. A transplantable human carcinoid as model for somatostatin receptor-mediated and amine transporter-mediated radionuclide uptake. The American journal of pathology. 2001;158(2):745-55.
136. Kennedy A, Nag S, Salem R, Murthy R, McEwan AJ, Nutting C, et al. Recommendations for radioembolization of hepatic malignancies using yttrium-90

microsphere brachytherapy: a consensus panel report from the radioembolization brachytherapy oncology consortium. International journal of radiation oncology, biology, physics. 2007;68(1):13-23.
137. Valkema R, Pauwels S, Kvols LK, Barone R, Jamar F, Bakker WH, et al. Survival and response after peptide receptor radionuclide therapy with [90Y-DOTA0,Tyr3]octreotide in patients with advanced gastroenteropancreatic neuroendocrine tumors. Seminars in nuclear medicine. 2006;36(2):147-56.
138. Kwekkeboom DJ, Mueller-Brand J, Paganelli G, Anthony LB, Pauwels S, Kvols LK, et al. Overview of results of peptide receptor radionuclide therapy with 3 radiolabeled somatostatin analogs. Journal of nuclear medicine : official publication, Society of Nuclear Medicine. 2005;46 Suppl 1:62s-6s.
139. Imhof A, Brunner P, Marincek N, Briel M, Schindler C, Rasch H, et al. Response, survival, and long-term toxicity after therapy with the radiolabeled somatostatin analogue [90Y-DOTA]-TOC in metastasized neuroendocrine cancers. Journal of clinical oncology : official journal of the American Society of Clinical Oncology. 2011;29(17):2416-23.
140. Baum RP, Kulkarni HR, Singh A, Kaemmerer D, Mueller D, Prasad V, et al. Results and adverse events of personalized peptide receptor radionuclide therapy with (90)Yttrium and (177)Lutetium in 1048 patients with neuroendocrine neoplasms. Oncotarget. 2018;9(24):16932-50.
141. Wangberg B, Westberg G, Tylen U, Tisell L, Jansson S, Nilsson O, et al. Survival of patients with disseminated midgut carcinoid tumors after aggressive tumor reduction. World journal of surgery. 1996;20(7):892-9; discussion 9.
142. Pauwels S, Barone R, Walrand S, Borson-Chazot F, Valkema R, Kvols LK, et al. Practical dosimetry of peptide receptor radionuclide therapy with (90)Y-labeled somatostatin analogs. Journal of nuclear medicine : official publication, Society of Nuclear Medicine. 2005;46 Suppl 1:92s-8s.
143. Cremonesi M, Ferrari ME, Bodei L, Chiesa C, Sarnelli A, Garibaldi C, et al. Correlation of dose with toxicity and tumour response to (90)Y- and (177)Lu-PRRT provides the basis for optimization through individualized treatment planning. European journal of nuclear medicine and molecular imaging. 2018.
144. Andersson P, Forssell-Aronsson E, Johanson V, Wangberg B, Nilsson O, Fjalling M, et al. Internalization of indium-111 into human neuroendocrine tumor cells after incubation with indium-111-DTPA-D-Phe1-octreotide. Journal of nuclear medicine : official publication, Society of Nuclear Medicine. 1996;37(12):2002-6.
145. Qian ZR, Li T, Ter-Minassian M, Yang J, Chan JA, Brais LK, et al. Association Between Somatostatin Receptor Expression and Clinical Outcomes in Neuroendocrine Tumors. Pancreas. 2016;45(10):1386-93.
146. Kim HS, Lee HS, Kim WH. Clinical significance of protein expression of cyclooxygenase-2 and somatostatin receptors in gastroenteropancreatic neuroendocrine tumors. Cancer research and treatment : official journal of Korean Cancer Association. 2011;43(3):181-8.
147. Pinato DJ, Tan TM, Toussi ST, Ramachandran R, Martin N, Meeran K, et al. An expression signature of the angiogenic response in gastrointestinal

neuroendocrine tumours: correlation with tumour phenotype and survival outcomes. British journal of cancer. 2014;110(1):115-22.
148. Kaemmerer D, Peter L, Lupp A, Schulz S, Sanger J, Prasad V, et al. Molecular imaging with (6)(8)Ga-SSTR PET/CT and correlation to immunohistochemistry of somatostatin receptors in neuroendocrine tumours. European journal of nuclear medicine and molecular imaging. 2011;38(9):1659-68.
149. Miederer M, Seidl S, Buck A, Scheidhauer K, Wester HJ, Schwaiger M, et al. Correlation of immunohistopathological expression of somatostatin receptor 2 with standardised uptake values in 68Ga-DOTATOC PET/CT. European journal of nuclear medicine and molecular imaging. 2009;36(1):48-52.
150. Brunner P, Jorg AC, Glatz K, Bubendorf L, Radojewski P, Umlauft M, et al. The prognostic and predictive value of sstr2-immunohistochemistry and sstr2-targeted imaging in neuroendocrine tumors. European journal of nuclear medicine and molecular imaging. 2017;44(3):468-75.
151. de Visser M, Verwijnen SM, de Jong M. Update: improvement strategies for peptide receptor scintigraphy and radionuclide therapy. Cancer biotherapy & radiopharmaceuticals. 2008;23(2):137-57.
152. Forssell-Aronsson E, Spetz J, Ahlman H. Radionuclide therapy via SSTR: future aspects from experimental animal studies. Neuroendocrinology. 2013;97(1):86-98.
153. Claringbold PG, Turner JH. Pancreatic Neuroendocrine Tumor Control: Durable Objective Response to Combination 177Lu-Octreotate-Capecitabine-Temozolomide Radiopeptide Chemotherapy. Neuroendocrinology. 2016;103(5):432-9.
154. Claringbold PG, Turner JH. NeuroEndocrine Tumor Therapy with Lutetium-177-octreotate and Everolimus (NETTLE): A Phase I Study. Cancer biotherapy & radiopharmaceuticals. 2015;30(6):261-9.
155. Kesavan M, Claringbold PG, Turner JH. Hematological toxicity of combined 177Lu-octreotate radiopeptide chemotherapy of gastroenteropancreatic neuroendocrine tumors in long-term follow-up. Neuroendocrinology. 2014;99(2):108-17.
156. Hassa PO, Haenni SS, Elser M, Hottiger MO. Nuclear ADP-ribosylation reactions in mammalian cells: where are we today and where are we going? Microbiology and molecular biology reviews : MMBR. 2006;70(3):789-829.
157. Tan B, Young DA, Lu ZH, Wang T, Meier TI, Shepard RL, et al. Pharmacological inhibition of nicotinamide phosphoribosyltransferase (NAMPT), an enzyme essential for NAD+ biosynthesis, in human cancer cells: metabolic basis and potential clinical implications. The Journal of biological chemistry. 2013;288(5):3500-11.
158. Tolstikov V, Nikolayev A, Dong S, Zhao G, Kuo MS. Metabolomics analysis of metabolic effects of nicotinamide phosphoribosyltransferase (NAMPT) inhibition on human cancer cells. PloS one. 2014;9(12):e114019.
159. Olesen UH, Christensen MK, Bjorkling F, Jaattela M, Jensen PB, Sehested M, et al. Anticancer agent CHS-828 inhibits cellular synthesis of NAD. Biochemical and biophysical research communications. 2008;367(4):799-804.

160. Chan M, Gravel M, Bramoulle A, Bridon G, Avizonis D, Shore GC, et al. Synergy between the NAMPT inhibitor GMX1777(8) and pemetrexed in non-small cell lung cancer cells is mediated by PARP activation and enhanced NAD consumption. Cancer research. 2014;74(21):5948-54.
161. Hovstadius P, Larsson R, Jonsson E, Skov T, Kissmeyer AM, Krasilnikoff K, et al. A Phase I study of CHS 828 in patients with solid tumor malignancy. Clinical cancer research : an official journal of the American Association for Cancer Research. 2002;8(9):2843-50.
162. Ravaud A, Cerny T, Terret C, Wanders J, Bui BN, Hess D, et al. Phase I study and pharmacokinetic of CHS-828, a guanidino-containing compound, administered orally as a single dose every 3 weeks in solid tumours: an ECSG/EORTC study. European journal of cancer (Oxford, England : 1990). 2005;41(5):702-7.
163. Scott CL, Swisher EM, Kaufmann SH. Poly (ADP-ribose) polymerase inhibitors: recent advances and future development. Journal of clinical oncology : official journal of the American Society of Clinical Oncology. 2015;33(12):1397-406.
164. Purohit NK, Shah RG, Adant S, Hoepfner M, Shah GM, Beauregard JM. Potentiation of (177)Lu-octreotate peptide receptor radionuclide therapy of human neuroendocrine tumor cells by PARP inhibitor. Oncotarget. 2018;9(37):24693-706.
165. Wangberg B, Ahlman H, Tylen U, Nilsson O, Hermodsson S, Hellstrand K. Accumulation of natural killer cells after hepatic artery embolisation in the midgut carcinoid syndrome. British journal of cancer. 1995;71(3):617-8.
166. Tomozawa Y, Jahangiri Y, Pathak P, Kolbeck KJ, Schenning RC, Kaufman JA, et al. Long-Term Toxicity after Transarterial Radioembolization with Yttrium-90 Using Resin Microspheres for Neuroendocrine Tumor Liver Metastases. Journal of vascular and interventional radiology : JVIR. 2018;29(6):858-65.
167. Memon K, Lewandowski RJ, Mulcahy MF, Riaz A, Ryu RK, Sato KT, et al. Radioembolization for neuroendocrine liver metastases: safety, imaging, and long-term outcomes. International journal of radiation oncology, biology, physics. 2012;83(3):887-94.
168. Toesca DAS, Ibragimov B, Koong AJ, Xing L, Koong AC, Chang DT. Strategies for prediction and mitigation of radiation-induced liver toxicity. Journal of radiation research. 2018;59(suppl_1):i40-i9.
169. Sangro B, Gil-Alzugaray B, Rodriguez J, Sola I, Martinez-Cuesta A, Viudez A, et al. Liver disease induced by radioembolization of liver tumors: description and possible risk factors. Cancer. 2008;112(7):1538-46.
170. Cui Y, Zhang XP, Sun YS, Tang L, Shen L. Apparent diffusion coefficient: potential imaging biomarker for prediction and early detection of response to chemotherapy in hepatic metastases. Radiology. 2008;248(3):894-900.
171. Koh DM, Scurr E, Collins D, Kanber B, Norman A, Leach MO, et al. Predicting response of colorectal hepatic metastasis: value of pretreatment apparent diffusion coefficients. AJR American journal of roentgenology. 2007;188(4):1001-8.
172. Padhani AR, Liu G, Koh DM, Chenevert TL, Thoeny HC, Takahara T, et al. Diffusion-weighted magnetic resonance imaging as a cancer biomarker: consensus and recommendations. Neoplasia (New York, NY). 2009;11(2):102-25.

173. Wang J, Takashima S, Takayama F, Kawakami S, Saito A, Matsushita T, et al. Head and neck lesions: characterization with diffusion-weighted echo-planar MR imaging. Radiology. 2001;220(3):621-30.
174. Surov A, Meyer HJ, Wienke A. Associations between apparent diffusion coefficient (ADC) and KI 67 in different tumors: a meta-analysis. Part 1: ADCmean. Oncotarget. 2017;8(43):75434-44.
175. Surov A, Meyer HJ, Wienke A. Correlation between apparent diffusion coefficient (ADC) and cellularity is different in several tumors: a meta-analysis. Oncotarget. 2017;8(35):59492-9.
176. Liapi E, Geschwind JF, Vossen JA, Buijs M, Georgiades CS, Bluemke DA, et al. Functional MRI evaluation of tumor response in patients with neuroendocrine hepatic metastasis treated with transcatheter arterial chemoembolization. AJR American journal of roentgenology. 2008;190(1):67-73.
177. Baskar R, Dai J, Wenlong N, Yeo R, Yeoh KW. Biological response of cancer cells to radiation treatment. Frontiers in molecular biosciences. 2014;1:24.
178. Nonnekens J, van Kranenburg M, Beerens CE, Suker M, Doukas M, van Eijck CH, et al. Potentiation of Peptide Receptor Radionuclide Therapy by the PARP Inhibitor Olaparib. Theranostics. 2016;6(11):1821-32.
179. Nightingale K. Acoustic Radiation Force Impulse (ARFI) Imaging: a Review. Current medical imaging reviews. 2011;7(4):328-39.
180. Woo H, Lee JY, Yoon JH, Kim W, Cho B, Choi BI. Comparison of the Reliability of Acoustic Radiation Force Impulse Imaging and Supersonic Shear Imaging in Measurement of Liver Stiffness. Radiology. 2015;277(3):881-6.